

GLOBAL ANALYSIS OF THE PI3K SIGNALING PATHWAY

by
Muhammad Saddiq Zahari

A dissertation submitted to Johns Hopkins University in conformity with the
requirements for the degree of Doctor of Philosophy

Baltimore, Maryland
December, 2015

Abstract

The human oncogene *PIK3CA* is frequently mutated in human cancers. Two hotspot mutations in *PIK3CA*, E545K and H1047R, have been shown to regulate widespread signaling events downstream of AKT, leading to increased cell proliferation, growth, survival, and motility. Although many studies have associated *PIK3CA* mutations with features of transformation, a global and quantitative study of how mutant *PIK3CA* impacts the signaling networks and consequently transforms epithelial cells has not yet been described.

The goal for this thesis project was to systematically dissect the signaling pathways that are activated due to these *PIK3CA* mutations in a global manner utilizing the power of phosphoproteomics and mass spectrometry. To this end, we employed stable isotope labeling of amino acids in cell culture (SILAC) to precisely identify and quantify the phosphorylation changes that occur in an isogenic series of immortalized non-tumorigenic breast epithelial cell lines containing E545K and H1047R mutations. We performed two phosphopeptide enrichment methods, namely titanium dioxide (TiO₂) beads to enrich for mainly serine/threonine phosphorylated peptides and anti-phosphotyrosine antibody to enrich for tyrosine phosphorylated peptides followed by high resolution LC-MS/MS analysis.

From ~9000 unique phosphopeptides identified, we found that aberrant activation of PI3K pathway leads to increased phosphorylation of a surprisingly wide variety of kinases and downstream signaling networks. By integrating the phosphoproteomic data

with human microarray-based AKT1 kinase assays, we discovered and validated six novel AKT1 substrates. One of these substrates, cortactin, was found to be important in conferring the cells with invasion/migration advantage. Through mutagenesis studies, we demonstrated that phosphorylation of cortactin by AKT1 is important for mutant PI3K-enhanced cell migration and invasion. Although it is well understood that these mutations in *PIK3CA* result in hyperactivation of the serine/threonine kinase AKT, we also observed an unexpected widespread modulation of tyrosine phosphorylation levels of proteins in the mutant cells. In the tyrosine kinome alone, 29 tyrosine kinases were altered in their phosphorylation status. Many of the regulated phosphosites that we identified were located in the kinase domain or the canonical activation sites, indicating that these kinases and their downstream signaling pathways were activated. Our study demonstrates the utility of a quantitative and global approach to identify mutation-specific signaling events and to discover novel signaling molecules as readouts of pathway activation or potential therapeutic targets.

Advisor: Akhilesh Pandey, M.D., Ph.D.

Reader: Edward Gabrielson, M.D.

Acknowledgments

The successful completion of this thesis would not have been possible without the help and support of various people, to whom I am eternally grateful.

I would like to thank my sponsor, Majlis Amanah Rakyat (MARA) of the Government of Malaysia, who has graciously supported this educational experience.

I am deeply indebted to my advisor Dr. Akhilesh Pandey, who took the leap of faith in accepting me into his lab over four years ago. With his guidance, unending enthusiasm and unique way of mentoring, I have grown tremendously as a scientist. He has taught me to think critically, to question every result and outcome, and to strive to maintain the highest degree of excellence in every aspect of my scientific development. I consider myself extremely lucky to have had the incomparable experience of undertaking my graduate study under Akhilesh's tutelage.

I would like to express my eternal gratitude to my mentor, Dr. Xinyan Wu, who has taught me everything in the lab and with whom I share all of my projects. His patience and kind teaching style were invaluable in training me to be an accomplished experimentalist. He has inspired me to be a creative and careful scientist, but more importantly, he has taught me the importance of perseverance in testing hypotheses, especially when encountering countless failed experimental results.

I am deeply grateful to my thesis mentors Dr. Saraswati Sukumar, Dr. Edward Gabrielson and Dr. Natasha Zachara, who provided important guidance, support and advice. I would like to thank Ed for his willingness to read this dissertation. I would like to especially thank Natasha who also serves as my program advisor and who is always willing to answer questions, give advice, and offer helpful suggestions for any nagging problems that I might have had.

I am also thankful to the Pandey lab colleagues, past and present, whose support and help have made my experience in the lab especially pleasant and collegial. Special thanks to Dr. Christine Jelinek, my sounding board, life coach and friend, for her overwhelming support. Thank you to Dr. Min-Sik Kim, who is always willing to give helpful and constructive advice. I would also like to thank Dr. Raja Sekhar Nirujogi and Dr. Sneha Pinto who were always very helpful in running my samples on the mass spectrometer and assisting me with data analysis.

I am eternally grateful to my friends, near and far, who have made my time in Baltimore especially enjoyable and eventful. I would like to thank Naqib and Aisha, who have put their trust in me, and whose companionships I miss every single day. I am especially grateful to my partner in crime, Joseph Sand, who has gone through thick and thin with me and who has probably heard every imaginable complaint about failed experiments and disasters in the lab. His overwhelming support and understanding have kept me sane and pulled me through the struggle of graduate school.

And last but most importantly, I would like to thank my family who has been supportive throughout my life in everything that I do. My mom, my two sisters, my aunt, and my other extended family members, I dedicate this thesis to all of them.

Table of Contents

Abstract	ii
Acknowledgments	iv
Table of contents	vii
List of figures	viii
Chapter 1. Introduction	1
Chapter 2. Phosphoproteomic profiling of isogenic mutant <i>PIK3CA</i> knockin cell lines	5
Chapter 3. Identification of cortactin as a novel AKT substrate and its importance in mutant PI3K-enhanced cell migration and invasion	41
Chapter 4. Widespread modulation of the tyrosine phosphoproteome by <i>PIK3CA</i> mutations	61
Chapter 5. References	85
Curriculum vitae	101

List of Figures

Chapter 2

- Figure 1. Analysis of isogenic MCF10A cell lines with mutant *PIK3CA* knockin 30
- Figure 2. Phosphoproteomic analysis of MCF10A cells with *PIK3CA* mutations 31
- Figure 3. Results of phosphoproteomic profiling of MCF10A cells with *PIK3CA* mutations 32
- Figure 4. Phosphorylation regulation patterns in MCF10A, Ex9-KI/Ex20-KI and J124-treated Ex9-KI/Ex20-KI cells 33
- Figure 5. Modulation of phosphorylation of proteins by *PIK3CA* mutations 34
- Figure 6. Phosphorylation modulated proteins involved in pyrimidine metabolism and cellular migration/invasion 35
- Figure 7. Widespread modulation of the kinome observed in *PIK3CA* Ex9-KI cells 36
- Figure 8. Widespread modulation of the kinome observed in *PIK3CA* Ex20-KI cells 37
- Figure 9. Phosphorylation motifs regulated by *PIK3CA* mutations 38
- Figure 10. Kinase–substrate and protein–protein interaction networks 39

Figure 11.	Phosphorylation-regulated proteins involved in nuclear pore complex	40
------------	---	----

Chapter 3

Figure 1.	Integrative analysis for identification of novel AKT substrates	54
Figure 2.	Cortactin is a novel substrate of AKT	55
Figure 3.	Co-localization of cortactin with its interacting partner and AKT in <i>PIK3CA</i> cells	56
Figure 4.	Phosphorylation of cortactin in cancer cell lines with <i>PIK3CA</i> mutations	57
Figure 5.	Cortactin is important in conferring migration/invasion ability in cells with <i>PIK3CA</i> mutations	58
Figure 6.	AKT1-mediated phosphorylation on cortactin is important for migration/invasion induced by activation of PI3K	59
Figure 7.	A proposed model of enhancing invasiveness by oncogenic activation of PI3K-AKT signaling cascades and phosphorylation of cortactin	60

Chapter 4

Figure 1.	Phosphoproteomic analysis of MCF10A cells with <i>PIK3CA</i> mutations	79
Figure 2.	Phosphotyrosine profiling results of MCF10A with <i>PIK3CA</i> mutations	80
Figure 3.	Widespread modulation of the kinome by <i>PIK3CA</i> mutants	81
Figure 4.	Hyperphosphorylation of tyrosine kinases in the <i>PIK3CA</i> mutant cells	82
Figure 5.	Site-specific regulation of tyrosine kinases by <i>PIK3CA</i> mutations	83
Figure 6.	Validation of phosphoproteomic results	84

Chapter 1: Introduction

The phosphoinositide 3-kinases (PI3Ks) are a family of lipid kinases that regulate a number of important biological processes including cell growth, survival, proliferation, and differentiation (Vivanco and Sawyers, 2002). In mammals, there are three classes of PI3K that are distinct in their mechanisms of regulation, substrate specificity and structure. Class I PI3Ks are heterodimers composed of a regulatory subunit (p85) and a catalytic subunit (p110) that transduce signals from receptors such as G-protein-coupled receptors and receptor tyrosine kinases. Upon growth factor stimulation, the Src Homology 2 (SH2) domains of the p85 subunit bind to the phosphorylated tyrosine residue of the receptors, recruiting PI3K to the membrane. This binding results in the release of inhibition of p85 on the lipid kinase activity of p110, which is then free to phosphorylate the phosphatidylinositol (4,5)-bisphosphate (PIP₂) phospholipid to generate phosphatidylinositol (3,4,5)-trisphosphate (PIP₃) (Yu et al., 1998). The accumulation of PIP₃ results in membrane recruitment and activation of PH-domain containing proteins such as PDK1 and AKT. The activation of AKT initiates a slew of signaling events that ultimately result in cell proliferation, survival, growth, and motility. The mitogenic effects from the activation of this pathway are the reason why *PIK3CA*, the gene that encodes p110 α , has been found to be frequently mutated in human cancers. Many of the mutations in this gene result in the gain of function of PI3K to confer cells with oncogenic advantage.

Recent studies have shown that three activating mutations, E542K and E545K in the helical domain and H1047R in the kinase domain, can lead to downstream activation

of PDK1 and/or AKT to promote carcinogenesis and metastasis (Samuels et al., 2004; Sarbassov et al., 2005; Vasudevan et al., 2009). Studies have also suggested that mutations in the kinase or helical domains have distinct effects on PI3K downstream signaling events. Zhao and Vogt showed that binding to p85, the regulatory subunit of PI3K, is essential for transformation induced by the kinase domain *PIK3CA* mutant (H1047R) but not for transformation induced by mutations in the helical domain (E542K and E545K) (Zhao and Vogt, 2008). A more recent study further demonstrated that the helical domain mutant, but not the kinase domain mutant, could directly associate with insulin receptor substrate 1 without the mediation of p85, which is required for activation of wild-type *PIK3CA* or *PIK3CA* with kinase domain mutations (Hao et al., 2013). Clinical studies have shown that tumors with H1047R mutation exhibit a better response to PI3K/mammalian target of rapamycin (mTOR) inhibitors compared to those carrying helical domain mutations (Janku et al., 2013).

To dissect the signaling mechanisms underlying the mutant *PIK3CA*-induced transformation, through genetic engineering, we utilized a series of human cell lines that differ only in their *PIK3CA* allele status, containing either wild-type (wt) or mutant forms of *PIK3CA* at codon 545 or 1,047 (Gustin et al., 2009; Samuels et al., 2005). Both of these *PIK3CA* mutations can activate multiple downstream pathways, which confer the ability for growth factor-independent proliferation *in vitro* and metastatic capability *in vivo* (Gustin et al., 2009; Samuels et al., 2005). We also utilized a previously developed inhibitor, J124, a novel and specific inhibitor of *PIK3CA* activity (Schmidt-Kittler et al., 2010). Treatment with this inhibitor can dramatically reduce AKT activity and inhibit metastasis of cancer cells bearing *PIK3CA* mutations. In this study, we performed a mass

spectrometry-based phosphoproteomic analysis of a spontaneously immortalized non-tumorigenic breast epithelial cell line MCF10A along with two isogenic derivatives generated by knock-in of mutant alleles—one bearing the E545K mutation located in the helical domain in exon 9 and the other bearing the H1047R mutation located in the kinase domain in exon 20 of the *PIK3CA* gene (hereafter referred to as Ex9-KI and Ex20-KI) (Gustin et al., 2009).

Mass spectrometry-based phosphoproteomics has become a powerful tool for studying signaling networks in a global manner, especially in conjunction with stable isotope labelling by amino acids in cell culture (SILAC) for a precise quantitative readout (Harsha et al., 2008; Olsen et al., 2006; Ong et al., 2002). Using TiO₂-based phosphopeptide enrichment, we identified and quantified 8,075 unique phosphopeptides, of which 1,142 are more phosphorylated in *PIK3CA* mutant cells and undergo a decrease in their phosphorylation status when treated with J124, a specific inhibitor of *PIK3CA* gene product. We used protein microarrays as a complementary platform to validate direct AKT1 substrates in vitro. Integration of the data from phosphoproteomic analysis with that from protein microarrays led to identification of a number of previously uncharacterized signaling molecules that appear to be involved in oncogenic signaling mediated through mutation of *PIK3CA*. Most notably, our studies identified cortactin as a novel AKT1 substrate whose phosphorylation enhances migration and invasion, key downstream events of the *PIK3CA* and AKT1 activation (Wu et al., 2014). We also enriched for tyrosine phosphorylated peptides using anti-phosphotyrosine antibody prior to LC-MS/MS analysis and we observed a widespread modulation of the tyrosine kinome, signifying that there are unexpected crosstalks that occur between the primarily

serine-threonine kinase signaling through the PI3K-AKT pathway with tyrosine signaling pathways (Zahari et al., 2015). Our profiling study should serve as a useful resource for research as well as clinical studies involving development of novel therapeutic targets.

Chapter 2: Phosphoproteomic analysis of isogenic mutant *PIK3CA* knock-in cell lines

Introduction

Although many studies have associated *PIK3CA* mutations with features of transformation, a global and quantitative study of how mutant *PIK3CA* impacts the signaling networks and consequently transforms epithelial cells has not been previously described. Here, we have utilized stable isotope labeling of amino acids in cell culture (SILAC) in conjunction with high-resolution mass spectrometry to analyze the phosphoproteome alterations that occur due to the two hotspot, activating mutations in *PIK3CA*, E545K and H1047R. An isogenic knockin system along with a novel *PIK3CA*-specific inhibitor and high-resolution mass spectrometry-based quantitative phosphoproteomics provided tools for us to map the signal transduction pathways that are specifically modulated by *PIK3CA* mutations in a comprehensive manner. With this approach, we identified >8,000 unique phosphopeptides, and observed global elevation of phosphorylation levels that impacted many kinases in the human kinome as a result of mutant *PIK3CA*. We found activation of diverse signaling pathways that were both previously known and unknown to be activated downstream of PI3K signaling. Our data provide a foundation for delineating the transformational effects of *PIK3CA* in cancer and other physiological processes.

Experimental Procedures

Cell culture and reagents

Cell lines were grown in 5% CO₂ at 37 °C. The breast epithelial cell line MCF-10A and its *PIK3CA* mutant knockin cell lines, Ex9-KI and Ex20-KI were cultured in DMEM/F12 (1:1) supplemented with 5% horse serum, 20 ng/ml EGF for MCF10A parental cells and 0.2 ng/ml EGF for knockin cells. Also, 10 µg/ml insulin (Roche), 0.5 µg/ml hydrocortisone (Sigma), and 100 ng/ml cholera toxin (Sigma) were supplemented for all cells. In order to label cells with stable isotopic amino acids, MCF10A and *PIK3CA* mutation knock in cells were propagated in DMEM/F12 SILAC media with corresponding complete supplements but deficient in both L-lysine and L-arginine (Thermo Fisher Scientific) and supplemented with light lysine (K) and arginine (R) for light, ²H₄-K and ¹³C₆-R for medium state and ¹³C₆¹⁵N₂-K and ¹³C₆¹⁵N₄-R for heavy state labeling (Cambridge Isotope Laboratories). Cells were seeded at 80% confluence in 5% horse serum DMEM/F12 basal media overnight. Cells were pretreated for 3 hours with 0.2 ng/ml EGF that is close to the physiological concentration of EGF in serum 54 and followed by 30 minutes treatment of 500 ng/ml J124 or 0.05% DMSO as vehicle control before harvesting. Before harvesting, cells were checked under microscope to ensure the proper confluence and healthy status. The phase contrast images of cells before harvesting are shown in Figure 1A.

Immunoblotting and siRNA knockdown

Cells were harvested and lysed in modified RIPA buffer (50 mM Tris-HCl, pH 7.4, 150 mM NaCl, 1 mM EDTA, 1% Nonidet P-40, 0.25% sodium deoxycholate, and 1

mM sodium orthovanadate in the presence of protease inhibitors). Whole cell protein extracts were denatured and separated in NuPAGE gels (Invitrogen), transferred to nitrocellulose membranes, and probed with primary and horseradish peroxidase-conjugated secondary antibodies. The primary antibodies used are anti-p44/p42 MAPK (9102; Cell Signaling Technology), anti-phospho-p44/p42 MAPK-Thr202/Tyr204 (9106; Cell Signaling Technology), anti-AKT (9272; Cell Signaling Technology), anti-pAKT-Ser473/Thr308 (9271, 2965; Cell Signaling Technology), anti-ACLY (4332; Cell Signaling Technology), pACLY-Ser544 (4331; Cell Signaling Technology), pGSK3 β -Ser9 (5538; Cell Signaling Technology) GSK3 β Cell Signaling Technology (9832, Cell Signaling Technology), EPHA2 (3625; Epitomics), pEPA2-Ser897 (6347; Cell Signaling Technology), β -ACTIN (A5316, Sigma) and 4G10 (17132; Millipore). 50 nM siRNA (CACCAGGAGCAUAUCAACAUA) targeting cortactin (Qiagen) was used for transfections with RNAiMax (Invitrogen). Cells were harvested 48 hours post transfection for assessing knockdown efficiency or other follow-up experiments.

Trypsin digestion

Cell lysates were prepared in urea lysis buffer containing 20 mM HEPES pH 8.0, 9 M urea, 1 mM sodium orthovanadate, 2.5 mM sodium pyrophosphate, 1 mM β -glycerophosphate and 5mM sodium fluoride. The lysates were sonicated and cleared by centrifugation at $3,000 \times g$ at 4°C for 10 min. Protein estimation was carried out using BCA protein assays. Equal amounts of protein from three SILAC labeled states were mixed, reduced with 5 mM dithiothreitol and alkylated with 10 mM iodoacetamide. Lysates were diluted to less than 2 M urea final concentration in 20 mM HEPES (pH 8.0)

and incubated with TPCK-treated trypsin at 25°C overnight. The reaction was quenched using 1% trifluoroacetic acid. The protein digest was desalted using C18 reverse phase column (Waters, UK) and eluted peptides were lyophilized and subjected to phosphopeptide enrichment.

TiO₂-based phosphopeptide enrichment

Peptides were fractionated by strong cation exchange (SCX) chromatography as described earlier (Beausoleil et al., 2004). Briefly, 10 mg of lyophilized peptides mixture was resuspended in 1 ml of SCX solvent A (5 mM KH₂PO₄ pH 2.7, 30% ACN) and were separated on a PolySULPHOETHYL A column (5 µm, 200 Å, 200 × 9.4 mm; PolyLC Inc., Columbia, MD) with an increasing gradient of SCX solvent B (5 mM KH₂PO₄ pH 2.7, 30% ACN, 350 mM KCl) on an Agilent 1100 HPLC system. In total, 15 fractions were collected. Each fraction was subjected to TiO₂-based phosphopeptide enrichment as described earlier (Larsen et al., 2005). Briefly, TiO₂ beads were incubated with DHB solution (80% ACN, 1% TFA, 3% 2,5-dihydroxybenzoic acid (DHB)) for 4 hours at room temperature. Each fraction was resuspended in DHB solution and incubated with pretreated TiO₂ beads (5 mg). Phosphopeptide-bound TiO₂ beads were washed three times with DHB solution and twice with 40% ACN. Peptides were eluted three times with 40 µl of 2% ammonia into 10 µl of 20% TFA.

Liquid chromatography tandem mass spectrometry

LC-MS/MS analysis of enriched phosphopeptides was carried out using a reverse-phase liquid chromatography system interfaced with an LTQ-Orbitrap Velos mass spectrometer (Thermo Fisher Scientific). The peptides were loaded onto an analytical column (10 cm × 75 μm, Magic C18 AQ 5 μm, 120 Å) in 0.1% formic acid and eluted with a linear gradient from 5 to 60% ACN in 90 minutes. Precursor scans (FTMS) were acquired in the range of 350-1,700 m/z at 60,000 resolution at 400 m/z on an Orbitrap analyzer. Ten most abundant precursor ions from a survey scan were selected for HCD fragmentation (isolation width of 1.90 m/z; 35% normalized collision energy and activation time of 0.1 ms were allowed) and MS2 spectra were acquired at 15,000 resolution at 400 m/z on the Orbitrap analyzer.

Mass spectrometry data analysis

Proteome Discoverer (v 1.3; Thermo Fisher Scientific) suite was used for quantitation and database searches. The tandem mass spectrometry data were searched using Mascot (Version 2.2.0) and SEQUEST search algorithms against a Human RefSeq database (v 46 containing 33,249 entries) supplemented with frequently observed contaminants. For both algorithms, the search parameters included a maximum of one missed cleavage; carbamidomethylation of cysteine as a fixed modification; N-terminal acetylation, oxidation at methionine, phosphorylation at serine, threonine and tyrosine and SILAC labeling $^{13}\text{C}_6$, $^{15}\text{N}_2$ -lysine; $^2\text{H}_4$ -lysine; $^{13}\text{C}_6$ -arginine and $^{13}\text{C}_6$, $^{15}\text{N}_2$ -arginine as variable modifications. The MS tolerance was set at 10 ppm and MS/MS tolerance to 0.1 Da. Score cut off was set to 0.01 false discovery rate at the peptide level. The probability of phosphorylation for each Ser/Thr/Tyr site on each peptide was calculated by the

PhosphoRS algorithm (Taus et al., 2011). We averaged the intensities of phosphopeptides identified from the forward and reverse experimental groups. We chose a 1.5 fold cut off to consider peptides as phosphorylation increased and a 0.67 fold for peptides to be considered as phosphorylation decreased. This threshold was chosen because we observed that AKT phosphorylation increased by 1.53 fold in *PIK3CA* mutant knockin cells. Many of the known phosphorylation sites of AKT substrates were found to range between 1.5 and 2-fold in the knock-in cell lines compared to the parental cells. Among these were BAD S75 (1.82), CTNNB1 S552 (1.62), HSPB1 S82 (1.81), PDCD4 S457 (1.50), PEA15 S116 (1.60), RANBP3 S126 (1.96) and YAP1 S127 (1.65). To identify and plot the differentially regulated phosphopeptides, we averaged the intensity of each phosphopeptide detected from MCF10A, *PIK3CA* mutant knockin cells and knockin cells treated with PIK3CA inhibitor, J124. The relative ratio was calculated by dividing the intensity of each phosphorylated peptide over the average intensity of the corresponding peptide and used for plot. The mass spectrometry proteomics data have been deposited to the ProteomeXchange Consortium (<http://proteomecentral.proteomexchange.org>) via the PRIDE partner repository with the dataset identifier PXD000599.

Motif analysis

The surrounding sequence (7 amino acid residues on either side) for each identified phosphorylation site was extracted from the RefSeq database. For phosphorylation sites that were localized at the region of the N-or C-termini, the surrounding sequence could not be extended in this fashion were excluded from further motif analysis. The motif-x algorithm (<http://motifx.med.harvard.edu>) was used to extract

motifs. The significance threshold was set to $P < 1e-3$. The minimum occurrence of motif was set to 20 for pSer peptides against an IPI Human proteome background. The NetworkKIN (<http://networkin.info>) tool was used to identify predicted protein kinases for all phosphosites as substrates. These were further classified based on motifs identified by motif-X.

Kinase-substrate and protein interaction network analysis

Three major kinase substrate databases, HPRD (www.hprd.org), PhosphositePlus (www.phosphosite.org) and Phospho.ELM (www.phospho.elm.eu.org) and one comprehensive protein-protein interaction database MIMI (www.mimi.ncibi.org) were merged based on kinase-substrate and protein-protein interaction pairs. If the protein pairs had both kinase-substrate in interaction partnerships, only kinase-substrate relationship was retained. We mapped 474 proteins whose phosphorylation levels were directly correlated with PI3K activity, with the merged database. Only kinase-substrate and protein interactions between the proteins belonging to the searched data set were selected, thereby excluding external candidates. The resulting interactome contained 208 phospho-regulated proteins forming 144 kinase-substrate and 274 protein-protein interaction relationships. The network was visualized by Cytoscape in the mode of force-directed layout. A graph theoretical clustering algorithm, molecular complex detection (MCODE) (Bader and Hogue, 2003) was used to identify densely connected clusters.

Results

Phosphoproteomic analysis of mutant PIK3CA knock-in cells

To validate the system employed in this study, we first examined the phosphorylation levels of AKT1 and mitogen-activated protein kinase (MAPK) in the mutant cells, where we found phospho-AKT and phospho-MAPK levels to be dramatically elevated in both cells and substantially suppressed by J124 treatment (Figure 1B). To interrogate the aberrant signaling triggered by the mutations in *PIK3CA*, we combined SILAC and TiO₂-based phosphopeptide enrichment followed by liquid chromatography tandem mass spectrometry (LC-MS/MS) analysis. Lysates of MCF10A parental cells were mixed with Ex9-KI cells that were treated with vehicle or J124 in a 3-plex SILAC experiment (Figure 2A). The same experimental strategy was employed for the analysis of Ex20-KI cells in a separate 3-plex SILAC experiment (Figure 2B). After enrichment of phosphopeptides with TiO₂ beads, the samples were desalted and analyzed on a high-resolution Fourier transform mass spectrometer. We also carried out replicate experiments in which the SILAC labels were swapped. In all, we identified 8,075 unique phosphopeptides derived from 2,016 proteins. Of these, 7,199 phosphopeptides harbored serine phosphorylation, 1,631 phosphopeptides contained threonine phosphorylation and 168 phosphopeptides harbored tyrosine phosphorylation, and most of the phosphopeptides were singly or doubly phosphorylated (Figures 3A,B).

The SILAC ratios (KI cells versus MCF10A) of phosphopeptides obtained from the two replicate experiments of both *PIK3CA* knockin cells showed a strong positive correlation (the correlation coefficient $R=0.86$ for Ex9-KI group and $R=0.87$ for the Ex20-KI group) for two independent biological replicates (Fig. 3C,D). There were 2,469

phosphopeptides that were detected in common in the Ex9-KI and Ex20-KI experimental groups, and the SILAC ratios (Ex9-KI or Ex20-KI cells versus MCF10A) of these phosphopeptides in the two cells with *PIK3CA* mutations were also quite correlated ($R=0.70$) (Figure 3E). Of the 2,469 phosphopeptides detected in common, 826 peptides derived from 338 proteins demonstrated the same increased or decreased phosphorylation pattern (>1.5 -fold change in phosphopeptide intensity for both Ex9-KI and Ex20-KI cells) when compared with MCF10A cells. However, we also found that 417 peptides from 243 proteins were highly phosphorylated (>1.5 -fold change) only in Ex9-KI or Ex20-KI cells compared with MCF10A cells, but not in both. These changes in phosphorylation patterns suggest that although downstream signaling effects are largely similar for these two particular mutant forms of *PIK3CA*, there are also some that are unique to the individual *PIK3CA* mutations. For instance, we found three kinases, PAK2, PAK4 and SLK, that were highly phosphorylated only in Ex9-KI cells and have been reported to be activated by PI3K-AKT pathway to promote cell migration/ invasion (Roovers et al., 2009; Wells et al., 2002; Wilkes et al., 2005). It has been shown that breast cancer cells expressing *PIK3CA* with helical domain (Ex9) mutation are more invasive than the cells expressing *PIK3CA* with kinase domain (Ex20) mutations (Pang et al., 2009), which is consistent with the data from this isogenic knockin system. The evidence of increased phosphorylation of these kinases specific to each knockin mutant cell could shed new light on some of the mechanisms underlying the phenotypic differences induced by *PIK3CA* Ex9 or Ex20 mutants.

Global elevation of protein phosphorylation by mutant PIK3CA

Overall, we observed that introduction of a single oncogenic amino acid change (E545K or H1047R) in *PIK3CA* can substantially elevate protein phosphorylation levels. In both Ex9-KI and Ex20-KI experimental groups, four major regulation patterns were observed. The first pattern included phosphopeptides identified in the Ex9-KI and Ex20-KI experimental groups whose phosphorylation levels were 1.5-fold higher in mutant cells than parental cells and exhibited at least a 33% reduction in Ex9-KI/Ex20-KI cells on treatment with J124 (Figure 4A). A second pattern included peptides that were highly phosphorylated in Ex9-KI/Ex20-KI but were not substantially altered on treatment with J124 (Figure 4B). A third pattern was of peptides that were less phosphorylated in Ex9-KI/Ex20-KI but were not substantially altered on treatment with J124 (Figure 4C). The fourth pattern included a set of phosphopeptides whose phosphorylation levels were unaltered in knockin cells but underwent suppression on J124 treatment (Figure 4D). Overall, as compared with MCF10A cells, we observed increased phosphorylation of about 47% and 33% of peptides in Ex9-KI and Ex20-KI cells, respectively. To examine the effects of J124 on global protein phosphorylation, we generated an intensity plot depicting the distribution of \log_2 -transformed intensity ratios of highly phosphorylated peptides in Ex9-KI cells versus MCF10A cells, or J124-treated Ex9-KI cells versus MCF10A cells (Figure 5A). We observed that J124 treatment resulted in a significantly global shift of phosphorylation pattern in Ex9-KI cells and significantly reduced the phosphorylation levels of highly phosphorylated peptides identified in this study. A similar trend was observed in the case of Ex20-KI cells. This global trend was confirmed by western blot analysis using phospho-specific antibodies targeting some of the well-known key molecules downstream of the PI3K signaling pathway, including AKT1 and

GSK3 β and recently identified AKT1 substrates, ATP citrate lyase (ACLY) (Bauer et al., 2005; Berwick et al., 2002) and EPHA2 (Miao et al., 2009), which were elevated in knockin cells and were efficiently suppressed by J124 treatment (Figure 5B). These results clearly demonstrate that activation of mutated *PIK3CA* leads to a global increase in protein phosphorylation and profoundly affects signaling networks.

Activation of multiple signaling pathways by mutant PIK3CA

To better understand the global phosphorylation alterations induced by oncogenic *PIK3CA* mutations, we performed a Kyoto Encyclopedia of Genes and Genomes pathway analysis using an integrated online functional annotation tool, DAVID (Huang et al., 2009), for the proteins with increased phosphorylation in Ex9-KI and Ex20-KI cells. Representative signaling pathways that were significantly enriched ($P=0.05$) in *PIK3CA* mutant knockin cells and involved in the biological processes, including cytoskeleton and migration, kinase-regulated signaling and cell cycle regulation are shown in Figure 5C. In agreement with previously reported observations (Gustin et al., 2009), our global phosphoproteomic study revealed that multiple oncogenic kinase-regulated signaling pathways such as MAPK, mTOR and ErbB were highly phosphorylated and enriched in *PIK3CA* mutant knockin cells. We also observed that multiple cell cycle-related pathways were enriched in mutant knockin cells, which has been previously suggested to provide a proliferative advantage in basal cell culture medium (Gustin et al., 2009). Notably, one of the pathways among the cell cycle- and cell proliferation-related pathways pertains to pyrimidine metabolism. The link between activation of PI3K-AKT pathway and regulation of pyrimidine metabolism has been described in two recent

studies (Ben-Sahra et al., 2013; Robitaille et al., 2013). These studies demonstrated that mTOR signaling downstream of PI3K-AKT module could enhance the de novo pyrimidine synthesis through phosphorylation of Ser1859 on CAD (carbamoylphosphate synthetase 2, aspartate transcarbamylase and dihydroorotase), a site that was also detected as highly phosphorylated in our experiments. We also observed increased phosphorylation of four other key enzymes (CTPS, RRM2, TK1 and DUT), which are involved in pyrimidine metabolism (Figure 6A). Finally, pathways regulating cell migration and invasion, such as those mediating actin rearrangements, cell adhesion and tight junction networks, were also found to be enriched (Figure 5C and 6B).

Widespread modulation of phosphorylation of the kinome

Of the 972 proteins that were found to be highly phosphorylated by one or both *PIK3CA* mutants, 46 were protein kinases. Of these protein kinases, 39 and 30 kinases were highly phosphorylated at serine/threonine residues in Ex9-KI or Ex20-KI cells, respectively (22 in common), suggesting that PI3K has a broad role in regulating cellular protein kinase activity. To obtain a systematic view of these differentially phosphorylated kinases, we mapped them and the corresponding phosphorylation sites onto a phylogenetic tree of the human kinome (Figures 7 and 8). Many of these modulated kinases have been shown to be associated with oncogenic transformation or metastasis in diverse cancers. Of the 39 highly phosphorylated kinases detected in Ex9-KI cells, elevation in the phosphorylation level of 25 kinases could be reversed by a short treatment with J124, suggesting that these kinases are likely to be directly regulated by AKT and/or PDK. Consistent with this suggestion, increased phosphorylation of S21 on

GSK3A, S9 on GSK3B and S897 on EPHA2 is already known to be directly phosphorylated by AKT (Cross et al., 1995; Miao et al., 2009; Srivastava and Pandey, 1998) and phosphorylation of these sites is critical in regulation of their kinase activities (Huang et al., 2009; Miao et al., 2009; Pang et al., 2009). For instance, AKT has been recently shown to phosphorylate EPHA2 to induce ligand-independent activation of EPHA2 and to promote cell migration and invasion (Miao et al., 2009). In addition to increased phosphorylation of receptor tyrosine kinases, such as EGFR (T693) and EPHA2 (S897), we also observed increased phosphorylation on of a non-receptor tyrosine kinase, PTK2 (S932) also known as FAK1.

Phosphorylation motifs enriched in mutant PIK3CA cells

The preference of amino acid motifs surrounding the phosphorylation sites is one of the major mechanisms that contribute to kinase specificity (Ubersax and Ferrell, 2007). Identification of overrepresented motifs could help pinpoint upstream kinases activated by mutant *PIK3CA*. To determine which linear motifs were overrepresented in our data set, we used the motif-X algorithm (Figure 9A,B). The peptides whose phosphorylation was increased in Ex9-KI and Ex20-KI cells and reduced on treatment with J124 were selected for this analysis. We identified 15 significantly enriched pS motifs (Figure 9A) and the sequence logos of top four enriched motifs are depicted in Figure 9B. Among these enriched motifs, eight were basic-rich motifs while three resembled the minimal AKT substrate motifs (RxRxxpS or RxxpS), which were ranked as the top two enriched phosphorylation motifs by motif-X analysis and Figure 9C. Prediction of the kinases upstream of these regulated phosphopeptides using the NetworKIN algorithm led to

identification of 34 kinases. The fraction of phosphopeptides corresponding to substrate motifs of each kinase was calculated and plotted in a heat map (Figure 9B). In agreement with the results of analysis with motif-X, the AKT kinase family was predicted to target the basic-rich motifs that were enriched in our data set (Figure 9B). In the integrated heat map combining motif-X and NetworkKIN analysis, we observed that a large number of phosphopeptides contained sequence motifs that could be phosphorylated by RPS6K, a kinase downstream of mTOR, indicating activation of the canonical pathway from PI3K to AKT-mTOR-RPS6K. The activation of RPS6K is also supported by the fact that several phosphorylation-regulated sites known to be specifically phosphorylated by RPS6K were identified to be highly phosphorylated in *PIK3CA* mutant knockin cells. They are RPS6 S235/S240, EIF4B S442, HSPB1 S78/S82 and NCBP1 S22/T21. We also observed that CDK and MAPK kinases were predicted as the activated upstream kinases phosphorylating the peptides with the PxpSP substrate motif, (Figure 9B,C), consistent with our previous report (Gustin et al., 2009) that MAPK1 and MAPK3 were highly phosphorylated and activated in mutant *PIK3CA* knockin cells (Figure 1B). More importantly, of these upstream kinases, 11 (MAP4K4, MAPK1, PAK2, PAK4, PRKAA1, PRKCD, RPS6KA1, CDK2, CDK3, CSNK1A1 and AKT1) were indeed found to be more phosphorylated in *PIK3CA* mutant cells and were downregulated upon J124 treatment. In addition to the activation of canonical kinases (such as AKT1, RPS6K1 and MAPK1) by oncogenic *PIK3CA* mutations, identification of a broader spectrum of PI3K-modulated kinases, including PAK2/4, CASNK1A1, MAP4K4 and PRKCD, could bring new insights into the understanding of the mechanisms of oncogenic transformation induced by mutant *PIK3CA*.

Interactome analysis to identify activated kinase pathways

Our motif analysis indicated that kinases, including AKT, MAPKs and CDKs, were activated in *PIK3CA* mutant knock-in cells. To understand the signaling networks more fully, we decided to study the kinase–substrate relationships and protein–protein interactions among the identified phosphoproteins. To do so, we first generated a database by integrating three kinase–substrate databases, HPRD (Keshava Prasad et al., 2009), PhosphoSitePlus (Hornbeck et al., 2012) and Phospho.ELM (Dinkel et al., 2011), with a protein–protein interaction database (Jayapandian et al., 2007), which merges protein–protein interaction information obtained from well-known interaction databases, including HPRD (Keshava Prasad et al., 2009), BIND (Bader et al., 2003) and IntAct (Kerrien et al., 2012). After removing redundant entries, the final integrated database had 7,047 kinase–substrate pairs with 77,176 protein–protein interaction pairs. Next, we mapped 474 proteins whose phosphorylations were increased in *PIK3CA* mutant knockin cells and decreased on the treatment of J124, to our integrated protein–protein interaction networks. We identified 108 kinase–substrate and 310 protein–protein interaction pairs composed of 208 differentially phosphorylated proteins. There were 11 kinases that were regulated by PI3K but not mapped in the network. The main interaction networks were visualized using Cytoscape (Figure 10A). We then used a graph theoretic algorithm, molecular complex detection, to discover highly connected interaction clusters (Bader and Hogue, 2003). In Figure 10B-E, four of the top ranked interaction clusters are shown. Of note, in agreement with our phosphomotif enrichment analysis, phosphorylated MAPK1 and AKT1 (Figure 10B,C) form the central hubs of the two top-ranked networks. This suggests not only that AKT1 and MAPK1 kinases were activated by

oncogenic *PIK3CA* mutations, but also that their downstream proteins/targets were consequently modulated by increased phosphorylation.

In addition to these canonical pathways, there were two other clusters in the regulated phosphoprotein network. One cluster is centered around PRKCD, also known as protein kinase C- δ a ubiquitously expressed isoform of the novel protein kinase C family (Figure 10D). This kinase can regulate apoptosis in a cell type and stimulus-dependent manner (Zhao et al., 2012). The stability and activity of PRKCD has been shown to be increased by PDK1, a key kinase in the PI3K pathway (Le Good et al., 1998). The activity of PRKCD is regulated by phosphorylation on several sites—in this study, we identified two PRKCD phosphorylation sites, S202 and S204, which were tightly correlated with PI3K activity but not well characterized previously. Of note, the amino acid sequence adjacent to Ser204 phosphorylation site matches the minimal AKT substrate motif (RxxpS), suggesting that AKT1 could potentially directly regulate PRKCD through phosphorylation.

The other cluster in the regulated phosphoprotein network comprises ten nuclear proteins, of which six are either known components of the nuclear pore complex (NPC) or proteins associated with the complex (Figure 10E). In addition, we also detected ten other NPC or NPC-associated proteins, eight of which were highly phosphorylated in Ex9-KI and/or Ex20-KI cells (Figure 11). Of these PI3K-regulated phosphoproteins, multiple phosphosites identified in this study have also been identified in other contexts. For instance, phosphorylation of NUP98 S591, S595 and S606 by CDK1 or NEK6 is crucial for disassembly of the NPC during mitosis (Laurell et al., 2011). Although its

phosphorylation is not directly involved in NPC disassembly, RanGAP1 S428/442 is also a substrate for CDK1 (Swaminathan et al., 2004). Nup153 S516, which we identified to be regulated by PI3K, was one of multiple ERK1 phosphorylation sites identified in this protein (Kosako et al., 2009). ERK1 phosphorylation of Nup153 decreased recognition of a nuclear transport receptor. We also identified phosphorylation of RanBP3 S126 by AKT1; this modification was previously shown to regulate the Ran gradient and nuclear transport (Yoon et al., 2008). Aside from these previously characterized NPC protein phosphosites, the specific functional effects of increased phosphorylation on the majority of NPC and associated proteins regulated by PI3K (10 out of 14) remain elusive. Nonetheless, our findings strongly suggest the likelihood of important roles for PI3K pathway activation in regulating mitotic NPC disassembly and nucleocytoplasmic transport.

We were able to identify both classic and less-characterized networks that were regulated by the activation of PI3K pathway. Notably, in our global phosphoproteomic study, almost two-thirds of the regulated phosphoproteins whose phosphorylation patterns are correlated with PI3K/AKT activities could still not be mapped onto known kinase–substrate relationships or protein–protein interaction networks. It is worth noting that in addition to the well-known kinases such as AKTs and PDK1 involved in the canonical PI3K signaling, there are six different kinases also containing the pleckstrin homology domain that can bind to phosphatidylinositol 3,4,5-trisphosphate (PIP₃). Among these kinases, four are non-receptor tyrosine kinases belonging to TEC tyrosine kinase family, namely TEC, TIK, BMX and BTK. Recent studies demonstrated that mutant *PIK3CA* could indeed activate BMX and directly phosphorylate STAT3 on Y705

(Guryanova et al., 2011; Hart et al., 2011). In our study, we observed increased phosphorylation on S727 of STAT3 in our mutant Ex9-KI cells and treatment with J124 could reduce this phosphorylation. Besides these four tyrosine kinases, there are two serine/threonine kinases, TRIO and KALRN, which can also bind PIP₃ through pleckstrin homology domains. However, exactly how these two kinases are regulated by and involved in PI3K signaling remains unknown. In this regard, it is important to note that we found that TRIO phosphorylation on S2455, S2476 and S2477 was closely associated with the activity of PI3K in mutant *PIK3CA* Ex9-KI cells. Further studies on these non-canonical PIP₃-regulated kinases are necessary to interpret the profound alterations induced by mutant *PIK3CA*. The abundance of these novel PI3K-modulated phosphorylation events also indicates that our knowledge of this serine/threonine kinase-centered signaling cascade is still far from complete.

Discussion

Oncogenic mutations in *PIK3CA* gene have been reported in many human cancer types. Using a gene targeting approach to knockout either wt or mutant *PIK3CA* alleles in colorectal cancer cell lines, Samuels et al. (2005) have previously demonstrated that mutant *PIK3CA* selectively regulated the phosphorylation level of AKT and its downstream transcription factors FKHR and FKHL1. However, a comprehensive and quantitative analysis of how *PIK3CA* mutants globally impact signaling networks and consequently transform epithelial cells has not yet been reported. In this study, we employed an isogenic model system to characterize the signaling alterations induced by the knockin of two hotspot oncogenic *PIK3CA* mutations (E545K or H1047R) in a

spontaneously immortalized non-tumorigenic breast epithelial cell line, MCF10A. This system can model breast epithelial cell malignancy induced by *PIK3CA* mutations. Using this unique model system, we applied a comprehensive phosphoproteomic analysis to discern and quantify global activation of phosphorylation-mediated signaling networks caused by these two *PIK3CA* mutations. Based on our phosphoproteomic analysis, it is possible that the elevation of the phosphorylation of some proteins resulted from the increased protein expression or the accumulation of both increased protein abundance and phosphorylation level. More importantly, we also observed phosphorylation of more than a thousand peptides from 474 proteins to be increased in *PIK3CA* mutant knockin cells and reduced on the short-term treatment with the *PIK3CA* inhibitor, J124. These changes are probably regulated by phosphorylation induced by mutant *PIK3CA* and not through the increase of protein abundance. Among these phosphorylation-increased proteins, only a fraction (208/474) has been reported to be involved in signaling networks related to the canonical PI3K-AKT signaling pathway. To our knowledge, this study provides the most comprehensive survey of quantified signaling perturbations in phosphorylation resulting from oncogenic activation of mutant *PIK3CA*. These newly identified signaling events should increase our understanding of the oncogenic effects resulting from mutations in *PIK3CA* gene, especially for development of novel therapeutic strategies for cancers with *PIK3CA* mutations.

From this data set, we were able to demonstrate increased phosphorylation of many key enzymes involved in important signaling networks and cellular processes in this predominantly serine/threonine kinase-driven signaling network. For instance, we have demonstrated increased phosphorylation of several key tyrosine kinases (Fig. 3a). In

addition, we identified modulation of phosphorylation of an AKT substrate, ACLY, which is the primary enzyme synthesizing cytosolic acetyl CoA. Acetyl CoA is the essential precursor for fatty acids, mevalonate synthesis (Watson et al., 1969) and a major source for protein acetylation reactions, including histone acetylation (Wellen et al., 2009). Phosphorylation-induced activation of ACLY by oncogenic mutation of *PIK3CA* could have the potential to enhance de novo fatty acid synthesis and also to globally regulate chromatin architecture and gene transcription. We also observed increased phosphorylation of ubiquitin protein E3 ligase (UBR4, ubiquitin protein ligase E3 component n-recogin 4) and several ubiquitin-specific peptidases (USP10, USP24 and USP43) in mutant *PIK3CA* knockin cells and the increase phosphorylation was diminished on J124 treatment. Some of these (UBR4, USP10 and USP24) were reported to be involved in oncogenic transformation of epithelial cells (Nakatani et al., 2005; Yuan et al., 2010; Zhang et al., 2012). These data suggest that *PIK3CA* oncogenic mutations not only globally modulate protein phosphorylation but can also potentially regulate multiple other post-translational modifications via the cross-talk between kinases and other enzymes.

Figure legends

Figure 1. Analysis of isogenic MCF10A cell lines with mutant *PIK3CA* knockin. (A)

Phase-contrast photomicrographs of MCF10A, Ex9-KI and Ex20-KI cells seeded in DMEM-F12 with 5% horse serum overnight and treated with 0.2 ng/ml EGF for 3 hours and followed by 30 minutes treatment of 500 ng/ml J124. Scale bar: 50 μ m (B) Western blot analysis of phosphorylated AKT (pT308), total AKT, phosphorylated p42/44 MAPK (pThr202/Tyr204) and total p42/44 MAPK in MCF10A parental cells, Ex9-KI and Ex20-KI cells with or without J124 treatment.

Figure 2. Phosphoproteomic analysis of MCF10A cells with *PIK3CA* mutations. (A)

A schematic depicting the strategy used for quantitative phosphoproteomic profiling of *PIK3CA* Ex9 knockin mutant cells. (B) A schematic depicting the strategy used for quantitative phosphoproteomic profiling of *PIK3CA* EX20 knockin mutant cells.

Figure 3. Results of phosphoproteomic profiling of MCF10A cells with *PIK3CA*

mutations. (A) Number of phosphoserine (pSer), phosphothreonine (pThr) and phosphotyrosine (pTyr) sites identified in the study. (B) Distribution of single, double, triple and quadruply phosphorylated peptides identified is indicated. (C,D) Density scatter plot of \log_2 -transformed phosphopeptide ratios (Ex9-KI or Ex20-KI versus MCF10A) from two SILAC reverse-labeled biological replicates. (E) Density scatter plot of \log_2 -transformed phosphopeptide ratios (x axis: Ex9-KI versus MCF10A and y axis: Ex20-KI versus MCF10A). Pearson coefficient correlation (R) is indicated.

Figure 4. Phosphorylation regulation patterns in MCF10A, Ex9-KI/Ex20-KI and J124-treated Ex9-KI/Ex20-KI cells. (A-D) Representative MS spectra of modulated phosphopeptides corresponding to each regulation pattern type are shown along with the phosphopeptide sequences. (Left panel) Phosphorylation patterns in MCF10A, Ex9-KI and J124-treated Ex9-KI cells. (Right panel) Phosphorylation patterns in MCF10A, Ex20-KI and J124-treated Ex20-KI cells. Phosphopeptides with similar phosphorylation profiles were grouped into four major clusters.

Figure 5. Modulation of phosphorylation of proteins by *PIK3CA* mutations. (A) Distribution of log₂-transformed intensity ratios of phosphorylation increased peptides (Ex9-KI versus MCF10A, fold change >1.5). The *x* axis shows log₂-transformed phosphopeptide intensity ratios and the *y* axis shows the density. Blue represents the ratios of Ex9-KI to MCF10A cells, while red represents the ratio of J124-treated Ex9-KI to MCF10A cells. The *P*-value was calculated using a paired Student's *t*-test comparing the two distributions was 2.2E-16. (B) Western blottings to confirm the phosphorylation status of a subset of phosphoproteins using phospho-specific antibodies, along with western blottings using antibodies against total proteins. β-Actin served as loading control. (C) The number of regulated proteins found in enriched signaling pathways (Modified Fisher's exact *P*-value<0.05) are shown for three biological processes—cytoskeleton and migration, kinase-regulated signaling and cell cycle.

Figure 6. Phosphorylation modulated proteins involved in pyrimidine metabolism and cellular migration/invasion. (A) Phosphorylation-regulated key enzymes in pyrimidine metabolism pathway modified from KEGG. (B) The model highlights the

literature-curated interaction network of proteins identified in the current study involved in the regulation and assembly of tight junction, adherens junction and focal adhesion represented using PathVisio (<http://www.pathvisio.org/>). The protein-protein interaction and the catalysis information for these molecules are extracted from Human Protein Reference Database and Ingenuity pathway database. The phosphosites of proteins that are differentially regulated by the *PIK3CA* mutants and/or the *PIK3CA* inhibitor are distinguished. These phosphoproteins include tight junction assembly proteins such as TJP1, TJP2, and cortactin; proteins in focal adhesion complexes such as ITGB4, PTK2, TLN1, TIAM1, and filamins; adherens junction proteins such as CTNNB1, and LMO7. The map also represents the proteins identified to be involved in the assembly and regulation of the actin cytoskeleton such as myelin light chains, RhoGEFs, PAKs, SSH2, PRKCD, and the components of the RAS/RAF signaling pathway. The details of nodes and edges specified are indicated in the figure.

Figure 7. Widespread modulation of the kinome observed in *PIK3CA* Ex9-KI cells.

A phylogenetic tree (modified from Human Kinome Tree (Manning et al., 2002)) of protein kinases identified in Ex9-KI cells. Phosphorylation increased kinases are in orange and kinases identified but did not change in phosphorylation levels are in light green. A colour-coded site regulation pattern is shown in the form of a circle divided into two parts. The top half represents the fold change of phosphorylation sites identified in Ex9-KI cells compared with MCF10A, whereas the bottom half represents the fold change ratio between J124-treated Ex9-KI cells compared with untreated cells. Regulated kinases that are known to be AKT substrates are underlined.

Figure 8. Widespread modulation of the kinome observed in *PIK3CA* Ex20-KI cells.

A phylogenetic tree (modified from Human Kinome Tree (Manning et al., 2002)) of protein kinases identified in Ex20-KI cells. Hyperphosphorylated kinases are in orange and kinases identified, but not changed in phosphorylation, are in light green. A color-coded site regulation pattern is shown in the form of a circle divided into two parts. Top half represents the fold-change of phosphorylation sites identified in Ex20-KI cells compared to MCF10A, whereas the bottom half represents the fold change ratio between J124-treated Ex20-KI cells compared to untreated ones.

Figure 9. Phosphorylation motifs regulated by *PIK3CA* mutations. (A) Significantly

overrepresented linear phosphorylation motifs identified using Motif X program were indicated on the left of the panel. Phosphopeptides matching the motifs were used for prediction of their upstream kinases by NetworKIN program. Based on the total number of phospho-modulated peptides, percentage of the number of phosphopeptides as substrates of predicted kinases were calculated and demonstrated in the heatmap (right panel). (B) Sequence logos of overrepresented phosphoserine linear motifs enriched among the peptides whose phosphorylation levels were increased in Ex9-KI and/or Ex20-KI cells as compared with MCF10A cells.

Figure 10. Kinase–substrate and protein–protein interaction networks. (A) A

network of kinase-substrate and protein-protein interactions within stringently regulated phosphoproteins was generated using Cytoscape. The proteins are color-coded based on the relative abundance of phosphopeptides (Ex9-KI vs. MCF10A cells outer circle and Ex20-KI vs. MCF10A inner circle). The top four highly connected clusters that are

highlighted on the main network map with dark green circles: (B) MAPK, (C) AKT and (D) PRKCD centered kinase–substrate and protein–protein interaction clusters. (E) The cluster enriched with NPC proteins. The network of kinase–substrate and protein–protein interaction within stringently regulated phosphoproteins was generated using Cytoscape. Proteins are color-coded based on their ratios (Ex9-KI versus MCF10A cells outer circle and Ex20-KI versus MCF10A inner circle) of phosphosites.

Figure 11. Phosphorylation-regulated proteins involved in nuclear pore complex.

Figure depicts the components of the nuclear pore complex and the proteins in each of the components that were identified through the phosphoproteomic profiling with the annotated phosphorylation site ratios.

Figure 1

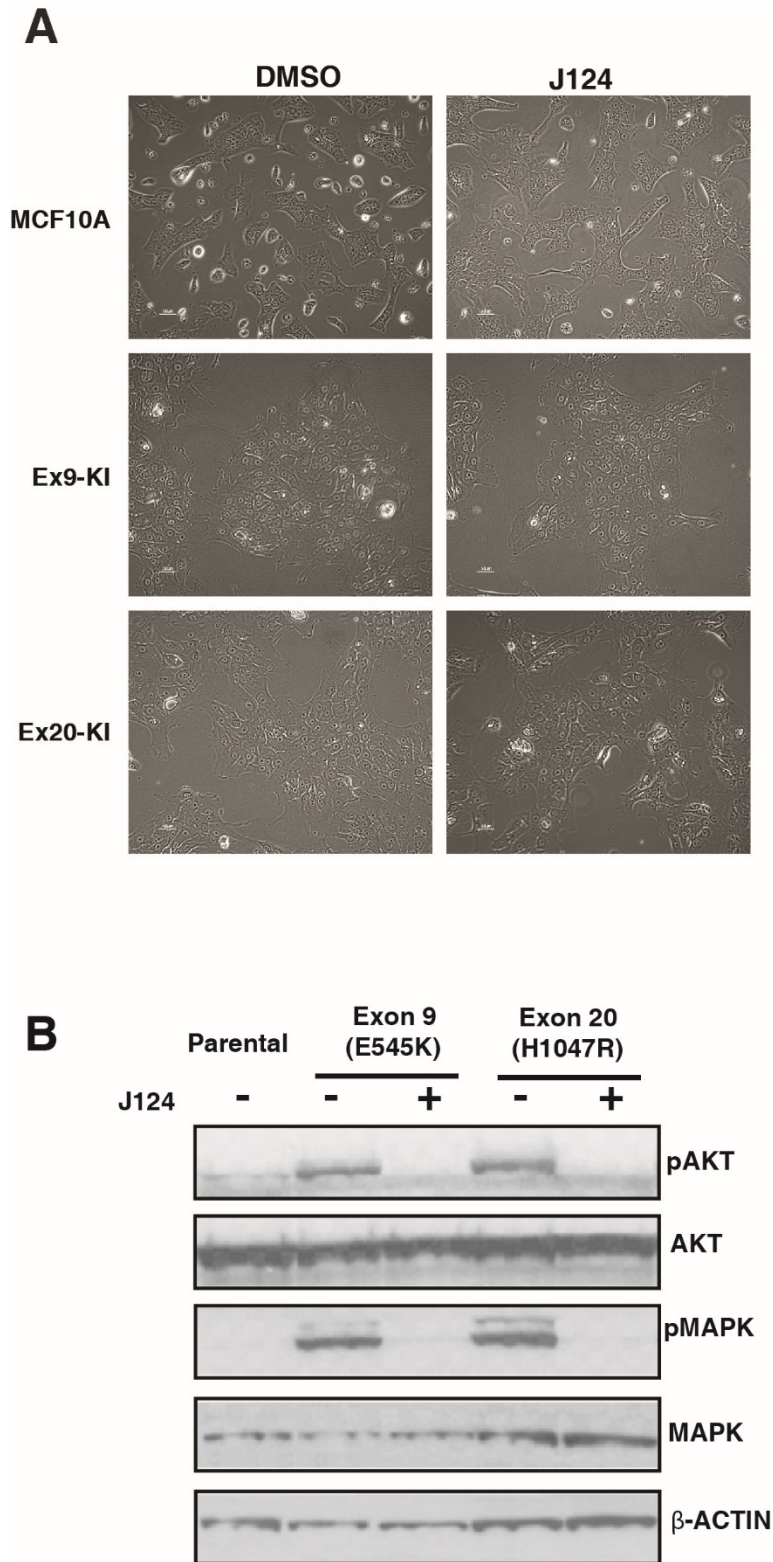


Figure 2

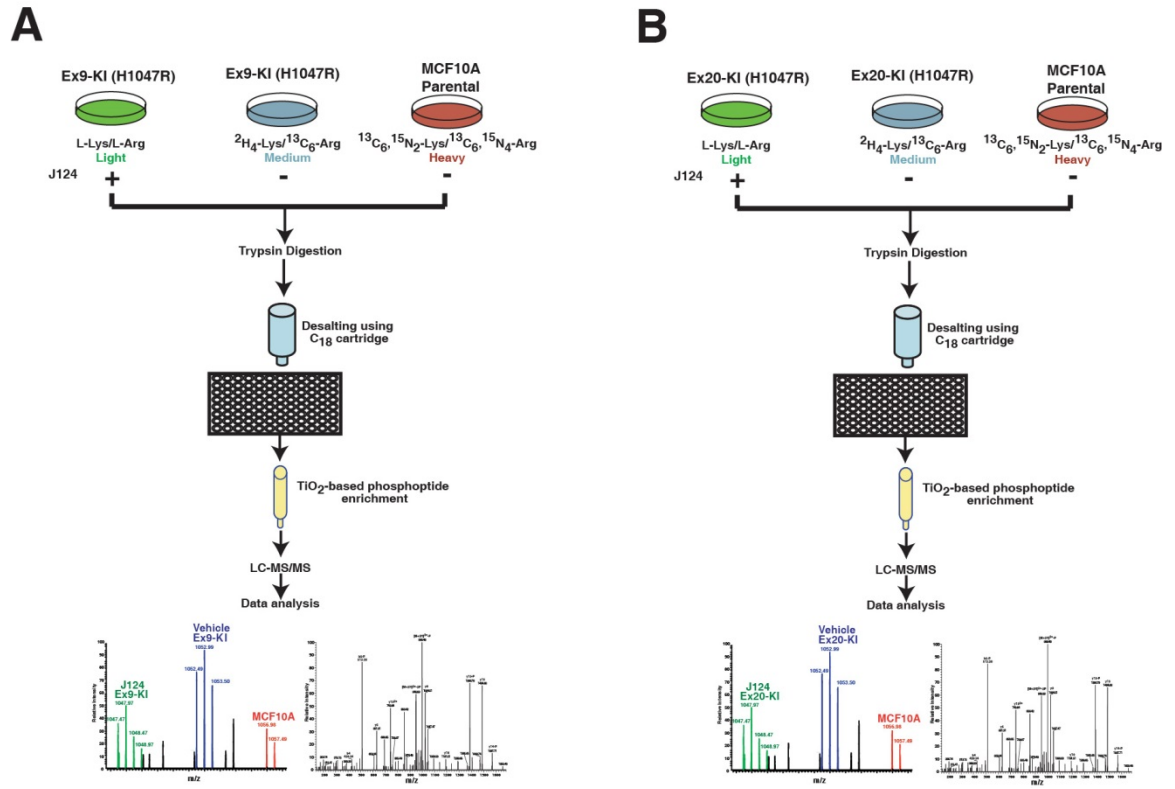


Figure 3

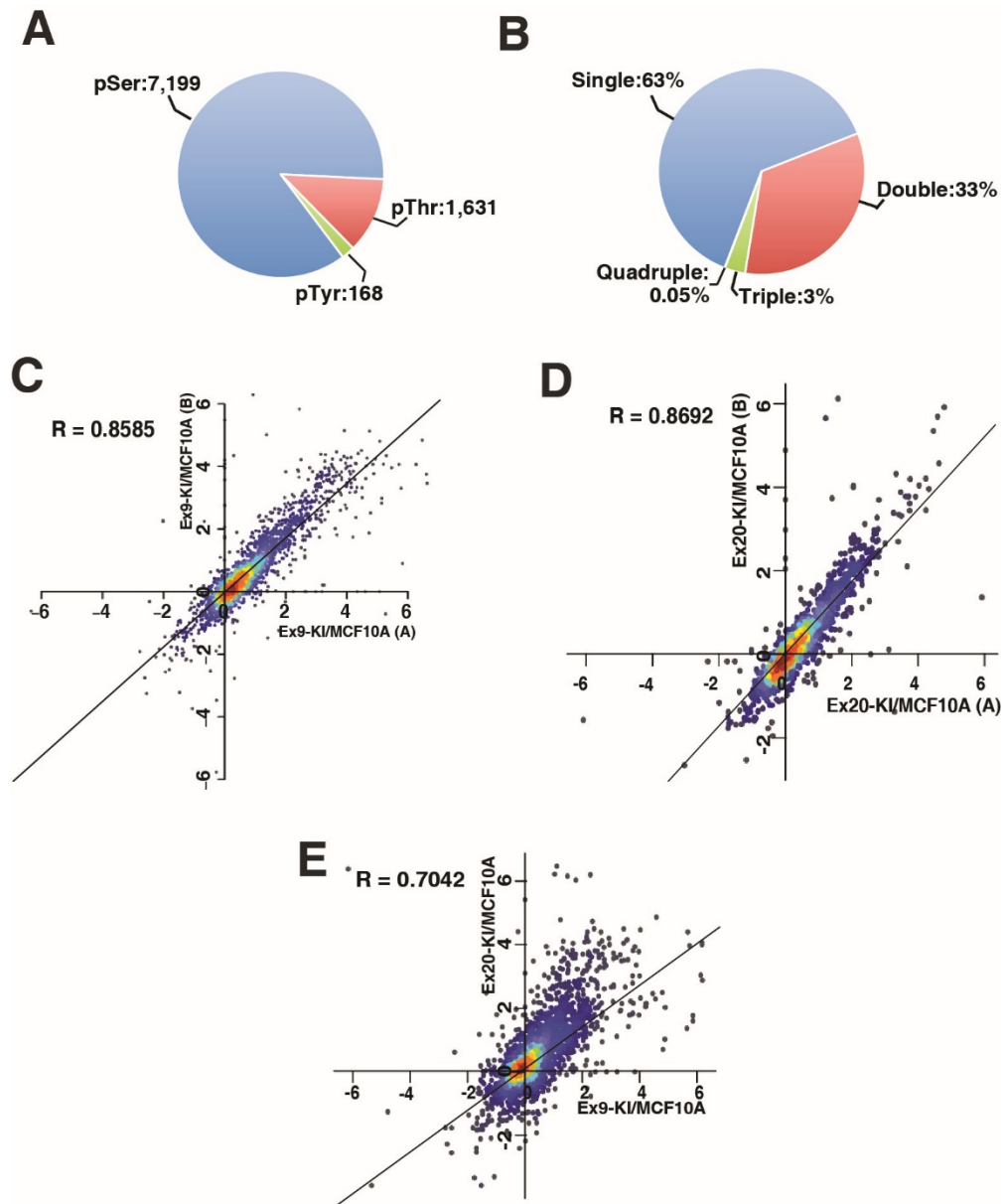


Figure 5

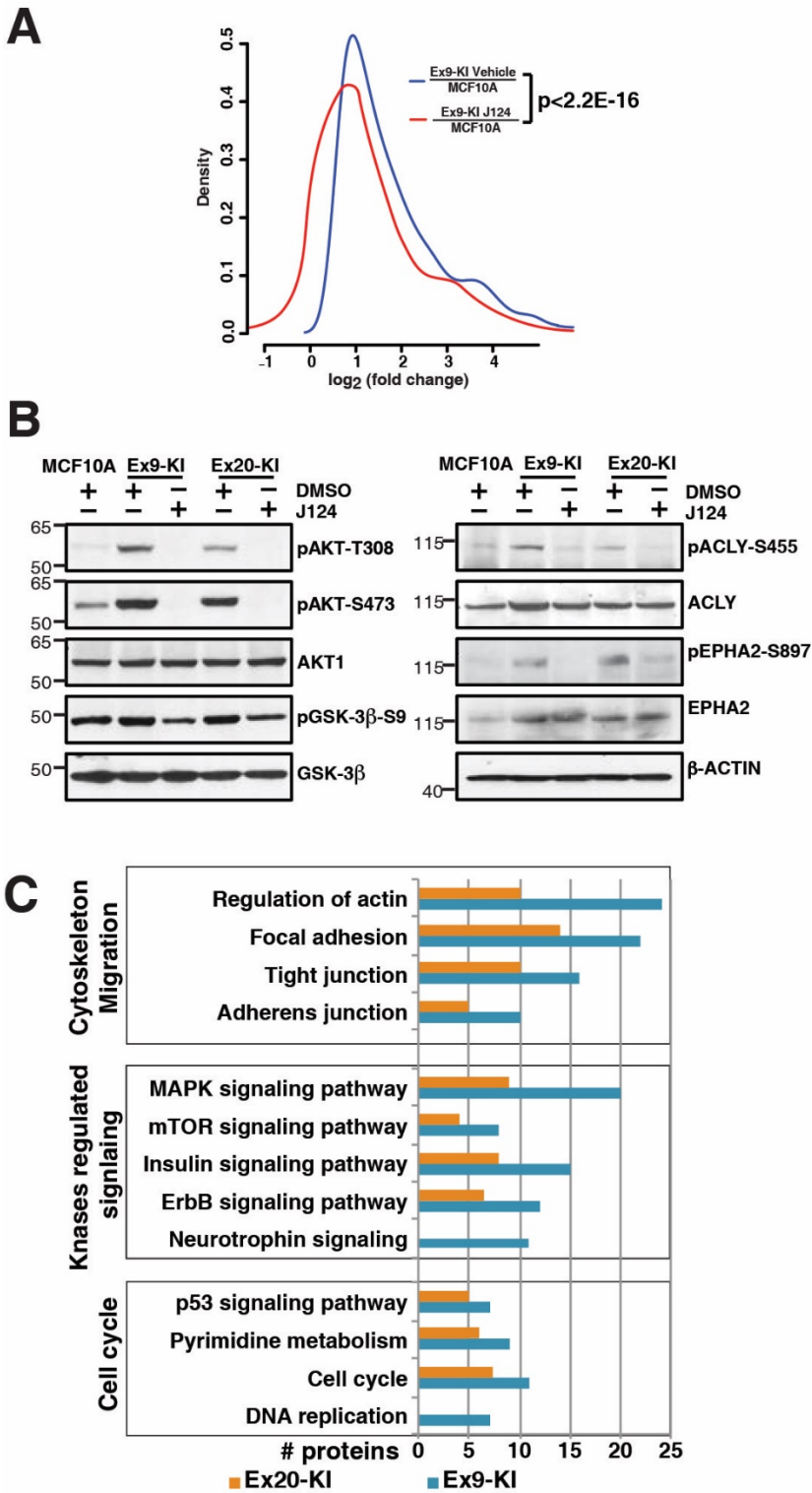
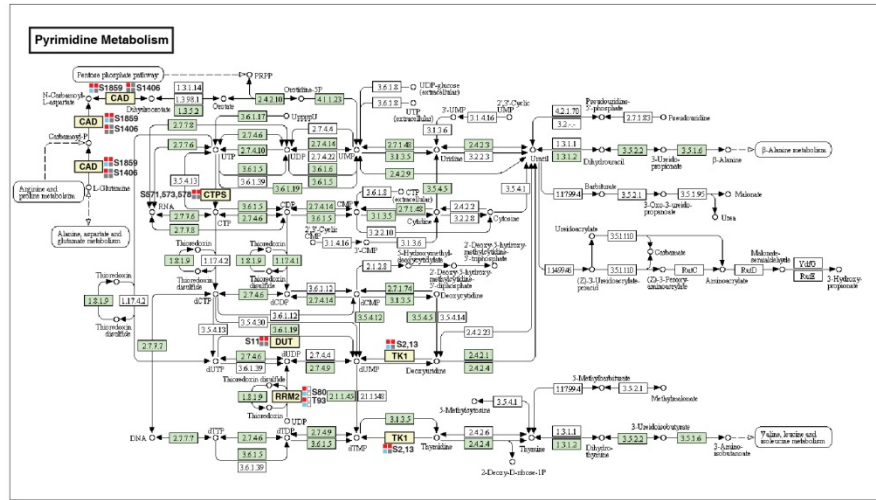


Figure 6

A



B

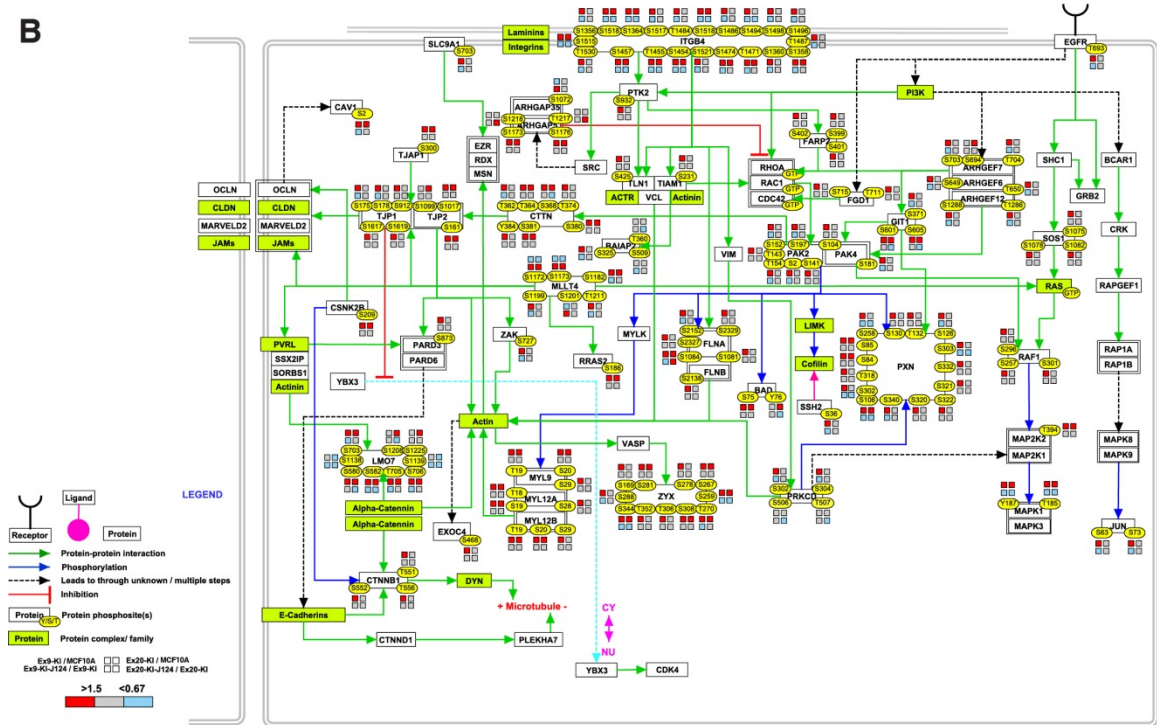


Figure 7

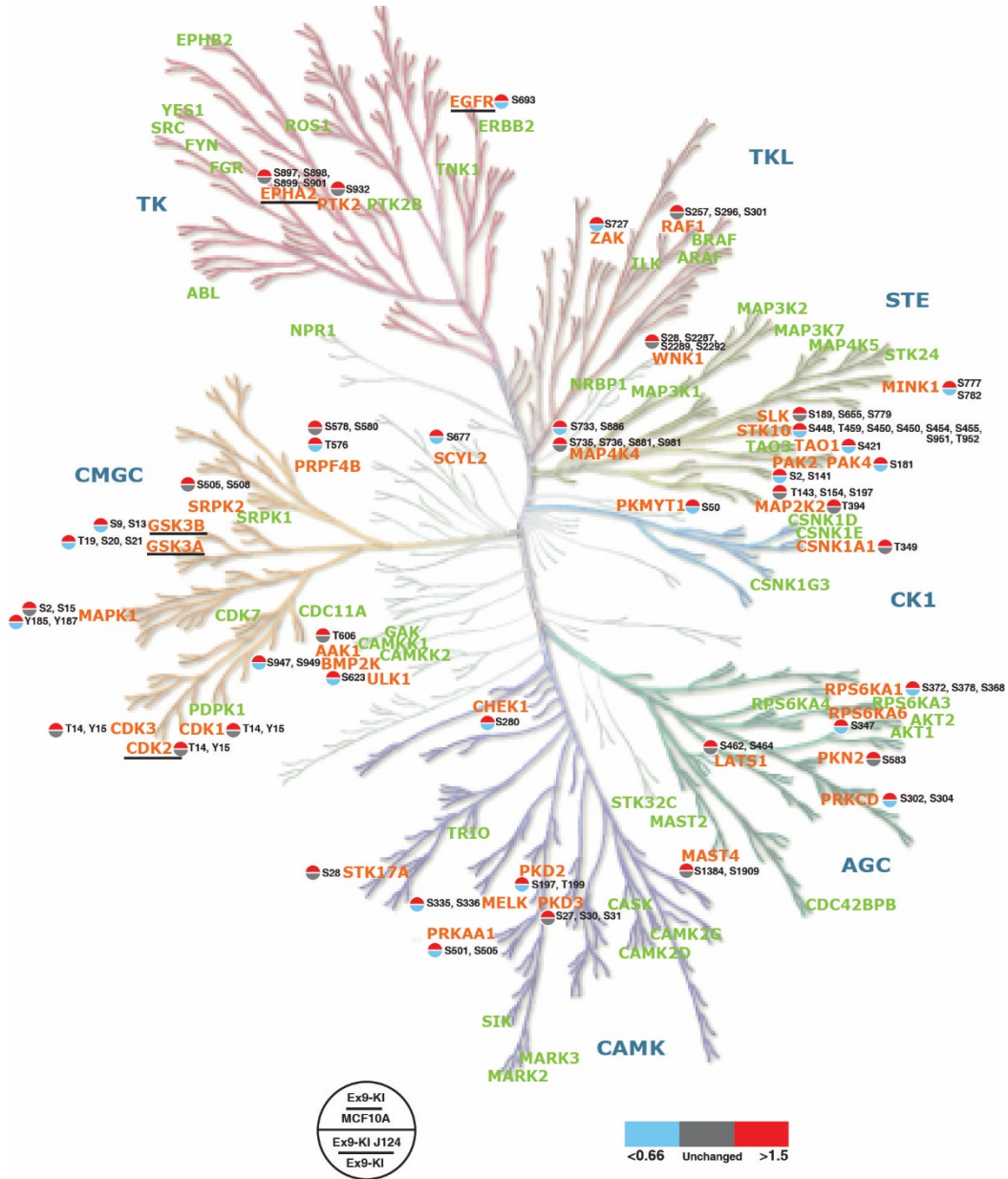


Figure 8

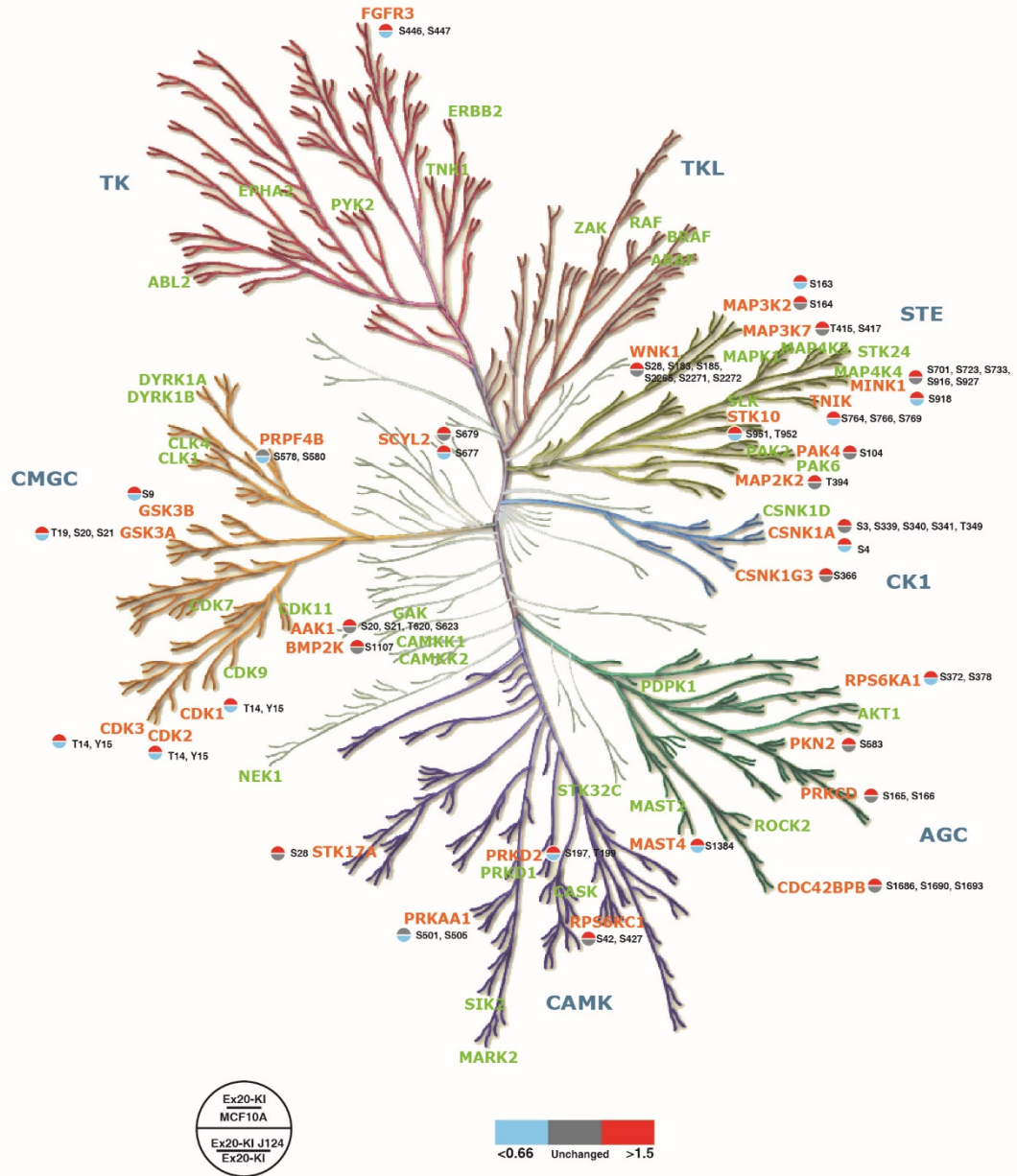


Figure 10

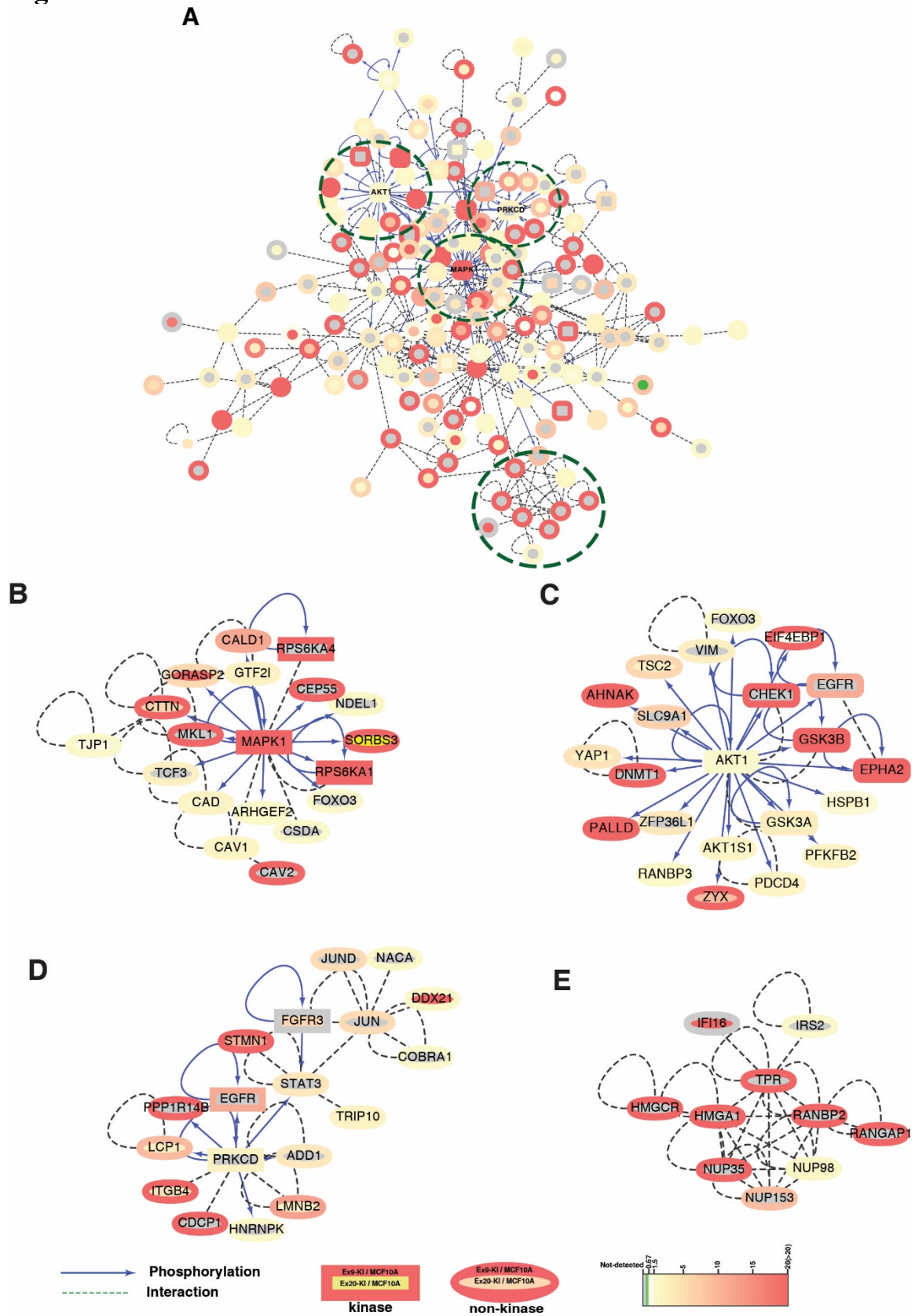
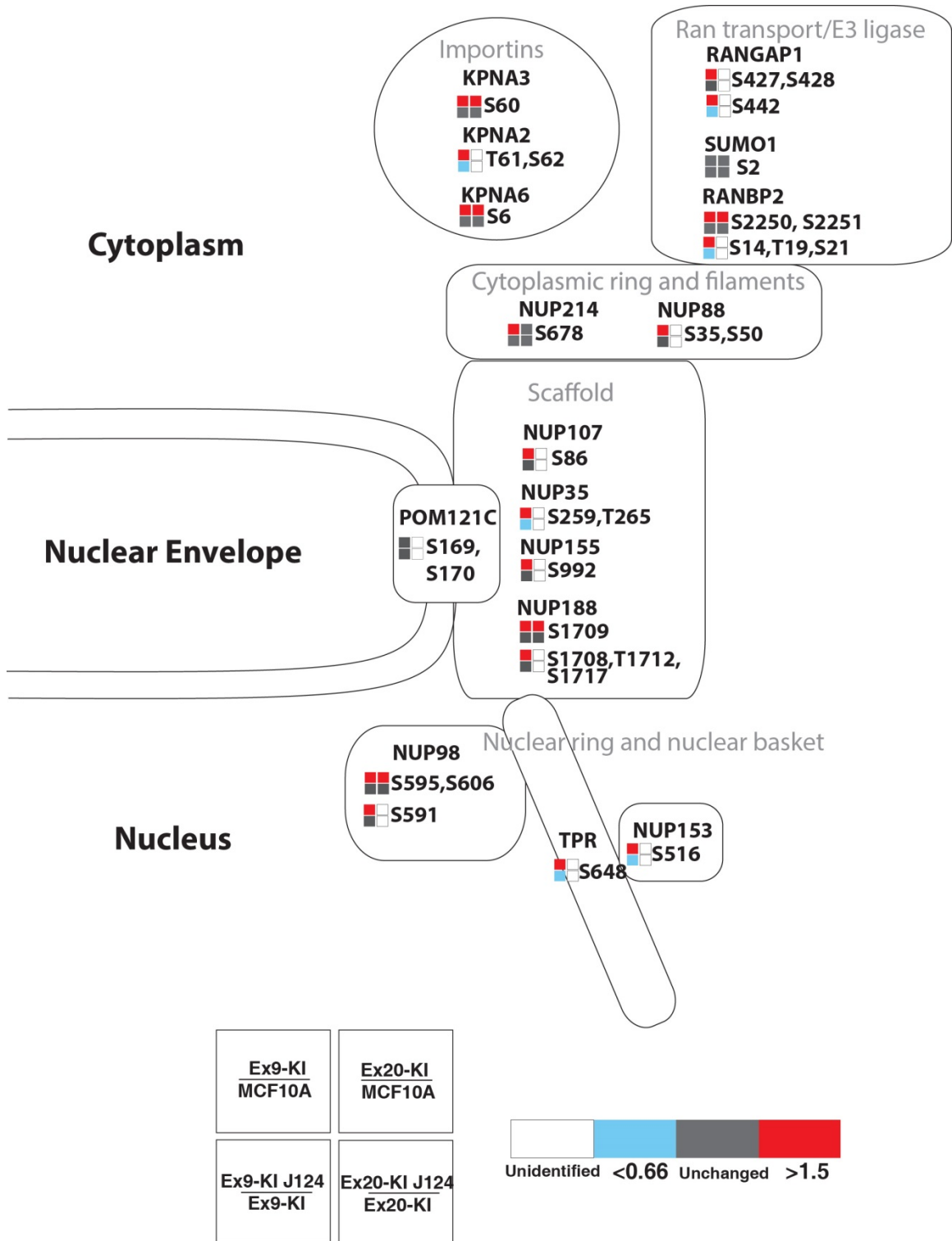


Figure 11



Chapter 3: Identification of cortactin as a novel AKT substrate and its importance in mutant PI3K-enhanced cell migration and invasion

Introduction

The major effector downstream of the activation of PI3K is the serine/threonine kinase AKT. Upon accumulation of PIP₃ in the inner plasma membrane generated by activated PI3K, AKT docks to PIP₃ via its pleckstrin homology (PH) domain. This position at the membrane primes AKT for phosphorylation by its activating kinases including PDK1 (which phosphorylates AKT at T308) and mTORC2 (which phosphorylates AKT at S473). The phosphorylation of these two activating sites leads to maximal activation of AKT which is then free to phosphorylate many downstream effector proteins. Over a hundred AKT substrates have been described, where the phosphorylation and activation of these proteins by AKT primarily result in cell growth, proliferation, survival and motility. Using the phosphoproteomics data that we generated in Chapter 2, we aimed to extend the list of AKT substrates to comprehensively understand the contribution of *PIK3CA* mutations in cancer. We also employed an *in vitro* kinase array using AKT1 in order to determine the *bona fide* AKT substrates. Overlay of both the phosphoproteomics and microarray data revealed six novel AKT substrates that have not been previously reported.

It was demonstrated that *PIK3CA* mutations can enhance cell migration and invasion of cancer cells (Samuels et al., 2005). AKT specifically has been shown to regulate motility, and hence the invasion/migration processes involved in cancer metastasis (Xue and Hemmings, 2013). Here, we showed that Ex9-KI and Ex20-KI cells are significantly more invasive than the wild type parental MCF10A cells, indicating that *PIK3CA* mutations cause increased invasive/migratory ability, consistent with previous reports. Analysis of the phosphoproteomics data generated in Chapter 2 revealed enrichment of signaling pathways regulating cell migration and cytoskeletal rearrangement in *PIK3CA* mutant knockin cells (Chapter 2, Figures 5C and 6B). Of the six confirmed novel direct substrates of AKT substrates, cortactin (CTTN) was of special interest because it is a component of the enriched pathways related to cell motility and cytoskeleton. Cortactin is a key branched actin regulator that regulates cell motility and transduces signals from the cell membrane to cytoskeletal proteins. Using mutagenesis and biochemical approaches, we demonstrated that phosphorylation of cortactin by AKT downstream of activated PI3K is essential in conferring cells with the enhanced invasion and migration ability.

Experimental procedures

Plasmids, site-directed mutagenesis and stable overexpression

Full-length cortactin CDS plasmids for isoform A and B were purchased from DNA Resource Core (Harvard) and subcloned into pBABE-puro vector. Site-directed mutagenesis for cortactin mutants was performed with QuikChange Site-Directed

Mutagenesis Kit (Agilent). HEK293T cells were used for retroviral package. Briefly, pBABE-cortactin wild type, mutant expression plasmids or control empty vector plasmids were co-transfected with pCL-Ampho (Imagenex) packing plasmid. Virus supernatants were collected and used for infection of MCF10A and knockin cells. Infected cells were then selected by 0.5ug/ml puromycin to obtain cells stably expressing cortactin proteins.

In vitro kinase assays

GST fusion proteins were generated in yeast or bacterial systems and purified with Glutathione-Sepharose beads. The GST-fusion proteins were pretreated with lambda phosphatase (NEB) at 30°C for 30 minutes and incubated at 60°C for another 30 minutes to inactivate any phosphatase activity. Pretreated GST-fusion proteins were mixed with ³²P-ATP (250 µCi) and with or without 100 ng AKT1 for 30 minutes at 30°C. The samples were resolved by SDS-PAGE and the proteins transferred onto nitrocellulose membranes. Phosphorylated and total proteins were visualized by autoradiography or MemCode staining (Thermo), respectively. To examine AKT1-induced phosphorylation sites, cortactin-GST fusion proteins were incubated with 1 mM ATP in the presence of absence of AKT1 at 30°C for 30 minutes. The samples were then resolved by SDS-PAGE and visualized by coomassie blue staining. Gel bands were excised and digested with trypsin. Tryptic peptides were extracted and analyzed on an LTQ-Orbitrap Elite mass spectrometer. Mass spectrometry data were searched against Human RefSeq with Sequest and Mascot algorithms.

Matrigel invasion assays

Cells were trypsinized and 5×10^4 cells seeded onto Biocoat matrigel invasion chambers (BD Biosciences) in 1% horse serum in DMEM/F12 medium for MCF10A cells, and serum-free media for DLD1 and BT20 cells. Complete medium was added in the lower chamber as chemoattractant. After 24 hours, the filter membranes were stained with DAPI (Invitrogen) and the number of cells that penetrated through the matrigel and membrane was counted in 10 randomly selected view fields at $20\times$ magnification.

Immunofluorescence analysis

Cells were seeded in 5% DMEM-F12 medium with 5% horse serum overnight and treated with 0.2 ng/ml EGF for three hours prior to fixation with 4% paraformaldehyde. Fixed cells were permeabilized with 0.05% Triton X-100 and blocked with 3% bovine serum albumin in phosphate-buffered saline. Cortactin was visualized with by immunofluorescence (IF) with anti-cortactin mAb 4F11 (Millipore) and Alexa Fluor 568 labeled goat anti-mouse IgG secondary antibody (Invitrogen). IF assays were also performed with rabbit monoclonal anti phosphorylated AKT (pS473) (4058, Cell Signaling Technology) antibody and rabbit polyclonal antibodies against WASP (SC-8350, Santa Cruz), NCK1 (ab23120, Abcam) and cofilin (SC-33779, Santa Cruz) followed Alexa fluor 488-labeled goat anti rabbit IgG secondary antibody (Invitrogen). The nucleus was stained with 4',6-diamidino-2-phenylindole (DAPI). Immunofluorescence analysis was carried out using a LSM710 confocal laser scanning microscope (Carl Zeiss).

Results

Identification of novel AKT substrates

Using the mass spectrometry-based phosphoproteomic approach, we identified 1,142 phosphopeptides (derived from 474 proteins) that were stringently correlated with *PIK3CA* and AKT activities (that is, more phosphorylated in knockin cells and less phosphorylated on J124 treatment). Of these, 358 phosphopeptides were derived from 204 proteins matching a minimal AKT substrate motif, R/KxxpS/T. When compared with the kinase substrate databases described above, 16 proteins were known AKT substrates, including well-studied molecules in AKT signaling such as GSK3A, GSK3B, AKT1S1, EPHA2 and PFKFB2. However, ~92% (188 of the 204 proteins) were not previously reported as AKT substrates. It is indeed possible that although they contain the AKT substrate motif, other kinases in addition to AKT may also be able to phosphorylate these proteins on the same residues *in vivo*. A definitive way to assess this possibility is to use *in vitro* phosphorylation reactions to capture the direct phosphorylation targets of AKT. We employed a human protein microarray with 4,191 unique, full-length human proteins belonging to 12 major protein families to perform phosphorylation reactions with recombinant human AKT1 proteins in the presence of [γ - 32 P]-ATP (Newman et al., 2013). In comparison with a negative control reaction in which AKT1 was omitted, we identified 316 proteins that could be directly phosphorylated by AKT1 *in vitro*. To maximize the advantages of the two high-throughput proteomic approaches and to increase the confidence of identification of novel AKT substrates, we overlaid our mass spectrometry-based phosphoproteomic data with protein microarray-based data set and

found six novel substrates that were regulated by PI3K in our *PIK3CA* mutation knockin cell line model and could also be directly phosphorylated in vitro by AKT1 in the protein microarray experiment (Figure 1A). To test whether these proteins were direct substrates of AKT1, we performed in vitro kinase reactions by mixing recombinant AKT1 with each of these six proteins (cortactin, TRIP10, PRKCD, PPP1R13L, EIF4B and C19ORF21) purified as glutathione S-transferase (GST) fusion proteins. All six proteins were phosphorylated by AKT1 (Figure 1B), which provides solid evidence that these six proteins are bona fide AKT substrates. Interestingly, we identified a highly interconnected cluster containing PRKCD as a hub in our kinase–substrate and protein–protein interaction network analysis (Chapter 2, Figure 10D). This integrative analysis allowed us to confirm that the enrichment of PRKCD-centred network is probably the result of elevated phosphorylation of PRKCD by AKT1.

It has previously been demonstrated that *PIK3CA* mutations can enhance cell migration and invasion of cancer cells (Samuels et al., 2005). Analysis of the phosphorylation data revealed enrichment of signaling pathways regulating cell migration and cytoskeletal rearrangement in *PIK3CA* mutant knockin cells (Chapter 2, Figures 5C and 6B). To investigate the effects of these phosphorylation-increased pathways in non-tumorigenic breast epithelial cells containing mutant alleles of *PIK3CA*, we employed matrigel-coated Boyden chamber assays to evaluate their invasive abilities. The results revealed that Ex9-KI and Ex20-KI cells could indeed penetrate matrigel to a much greater extent than the parental MCF10A cells. Moreover, the invasive ability enhanced by activation of *PIK3CA* could be dramatically attenuated by treatment with the *PIK3CA* inhibitor, J124, as well as by the AKT inhibitor IV (Figure 1C). Of the six confirmed

novel direct substrates of AKT substrates, cortactin (CTTN) was of special interest because it is a component of the enriched pathways related to cell motility and cytoskeleton (Chapter 2, Figures 5C and 6B). Cortactin is a key branched actin regulator that regulates cell motility and transduces signals from the cell membrane to cytoskeletal proteins. It is frequently overexpressed in advanced cancers and enhances cancer cell migration and invasion (MacGrath and Koleske, 2012), and ectopic overexpression of cortactin in head and neck squamous cell carcinoma cell lines has been reported to increase AKT activity (Timpson et al., 2007). As a key regulator of actin branching, the activity of cortactin activity is modulated by multiple kinases, including tyrosine kinases SRC and FYN, and serine/threonine kinases ERK1/2 and PAK1 (MacGrath and Koleske, 2012). Our phosphoproteomic studies revealed that phosphorylation of cortactin at S405/T401 and S417/S418 was regulated by the PI3K-AKT pathway (Figure 2A). These four phosphorylation sites are located within or close to the proline-rich domain of cortactin (Figure 2B), which contains many sites of tyrosine and serine phosphorylation regulated by different kinases⁴⁵. For instance, ERK kinase has been shown to phosphorylate cortactin on S405 and S418 (Martinez-Quiles et al., 2004). To confirm that AKT1 can also directly phosphorylate cortactin, we performed LC-MS/MS analysis of purified cortactin incubated in vitro with AKT1. This experiment confirmed that AKT is able to directly phosphorylate all four sites (S405/T401 and S417/S418) of cortactin (Figure 2C). To investigate whether cortactin and AKT interact in vivo, we performed immunofluorescence staining to examine the localization patterns of cortactin and phosphorylated AKT (pS473). As demonstrated in Figure 3A, we could clearly observe the co-localization of cortactin and phosphorylated AKT in Ex9-KI and Ex20-KI cells. It

is worth noting that the co-localization pattern was concentrated at the peripheral region of lamellipodia in Ex9-KI and Ex20-KI cells. We also performed immunofluorescence staining to examine the interaction between cortactin and its known partners in MCF10A, Ex9-KI and Ex20-KI cells. Cortactin largely co-localized with its interaction partners WASP, NCK1 and cofilin in all tested cell lines (Figure 3B-D). The co-localization patterns of cortactin and cofilin, NCK1 and WASP in peripheral membrane structures were only detected in Ex9-KI and Ex20-KI cells with *PIK3CA* mutations (Figure 3B-D).

To test whether phosphorylation of cortactin could also be regulated by AKT1 in other cells with alterations in the PI3K signaling pathway, we used another isogenic cell line pair derived from the colorectal cancer cell line DLD1 (Samuels et al., 2005). The parental line contained one wt *PIK3CA* allele and one mutant allele (E545K), and the two derivatives were created by homologous recombination so that one contained only the wt *PIK3CA* allele (DLD1-wt), while the other contained only the mutant allele (DLD1-mt). LC-MS/MS analysis was performed on anti-cortactin immunoprecipitates from cell lysates extracted from SILAC-labelled DLD1-wt (light) and DLD1-mt (heavy) cells (Figure 4A,B). This experiment showed that DLD1-mt cells had higher levels of phosphorylation of cortactin than DLD1-wt cells (Figure 4C). We also investigated a breast cancer cell line, BT20, harboring mutant *PIK3CA* alleles (Wu et al., 2005). Cell lysates from SILAC heavy-labelled BT20 cells treated with J124 or AKT inhibitor IV (AKT-IV) were mixed with untreated cells, then subjected to immunoprecipitation with anticortactin antibody (Figure 4A). LC-MS/MS analysis of immunoprecipitated cortactin again revealed that phosphorylation levels of cortactin were substantially reduced in BT20 cells treated with either J124 or AKT inhibitor IV (Figure 4D).

To further characterize the role of cortactin in promoting migration/invasion of *PIK3CA* mutant cells, we first employed small interfering RNA (siRNA) to knockdown cortactin expression in MCF10A, Ex9-KI and Ex20-KI cells (Figure 5A top panel). We found that knockdown of cortactin significantly reduced the invasive ability of *PIK3CA* mutant knockin cells (Figure 5A). A similar suppression of invasion was observed in DLD1-mt and BT20 cells after knockdown of cortactin expression (Figure 5B,C). We next wanted to determine the phosphorylation effect of cortactin on its function. Cortactin has been shown to possess three alternatively spliced isoforms encoding three different proteins that are 550, 513 or 634 amino acids long. To identify the predominant isoform(s) expressed in MCF10A cells, we conducted a database search against transcript databases in addition to carrying out reverse transcriptase-PCR using primers that could distinguish specific isoforms (Figure 6A). We found that transcripts of isoforms A and B, but not C, were detectable in MCF10A and mutant *PIK3CA* knockin cells. Thus, we cloned both of these isoforms into a retroviral expression vector and carried out site-directed mutagenesis to alter all four detected AKT1 phosphorylation sites (S405A, T401A, S417A and S418A). Wild-type and mutant versions of both cortactin isoforms (A and B) were stably expressed in parental MCF10A, Ex9-KI and Ex20-KI cells, as confirmed by western blot analysis (Figure 6B). Boyden chamber assays were employed to examine the effects of cortactin phosphorylation on cell migration and invasion where we found that overexpression of wt isoforms A and B promoted cell migration and invasion (Figure 6B), and this enhanced invasive capacity could be reduced by the treatment of AKT inhibitor (Figure 6D), suggesting that AKT-mediated phosphorylation of cortactin contributes to the invasive ability induced by overexpression of cortactin. In

contrast, overexpression of the mutant isoforms that could not be phosphorylated by AKT1 did not enhance, and perhaps even suppressed the migration and invasive ability of the cells (Figure 6B). Similar effects were observed in BT20 cells bearing *PIK3CA* mutations (Figure 6C). These studies, in aggregate, provide strong evidence that mutations of *PIK3CA* enhance the migration and invasiveness of cells through the activation of AKT and the subsequent phosphorylation of cortactin (Figure 7).

Discussion

Our integrated approach to identify kinase substrates by combining two high-throughput proteomic platforms—mass spectrometry-based phosphoproteomics and protein microarray-based kinase assays—enabled us to identify six novel AKT substrates. Functional studies confirmed that phosphorylation of one novel substrate, cortactin, is critical for migration/invasion induced by oncogenic activation of PI3K. Similar approaches employing high-throughput proteomic technology-based strategies can be applied to understand other cancer signaling pathways in a systematic manner. In summary, mutant PI3K-induced signaling events uncovered by our phosphoproteomic approaches along with the newly identified AKT1 substrates should be invaluable for research as well as clinical studies involving development of novel targeted therapies.

FIGURE LEGENDS

Figure 1. Integrative analysis for identification of novel AKT substrates. (A) Autoradiograph of novel AKT1 substrates identified from protein microarray-based AKT1 substrate assays. Left panel: autoradiographs of the reactions without AKT1; Right panel: autoradiograph of the reactions incubated with AKT1. (B) In vitro AKT1 kinase assays with indicated GST fusion proteins. Right panels: autoradiograph of ³²P-phosphorylated AKT1 substrates; left panels: Memcode staining of GST fusion proteins. (C) Matrigel migration/invasion assays for MCF10A, Ex9-KI and Ex20-KI cells treated with J124, AKT inhibitor IV or DMSO. Data are shown as mean±s.e.m. Mann–Whitney test was carried out to determine the statistical significance. The experiments were repeated twice.

Figure 2. Cortactin is a novel substrate of AKT. (A) Relative phosphorylation levels of cortactin phosphosites identified in SILAC-based phosphoproteomic analysis of Ex9-KI or Ex20-KI cells treated with or without J124 and parental MCF10A cells. (B) Domain structure of cortactin with phosphosites identified in this study. (C) Representative MS/MS spectra confirming phosphorylation of cortactin at T401, S405, S417 and S418 in *in vitro* AKT kinase–substrate assays followed by LC-MS/MS analysis.

Figure 3. Co-localization of cortactin with its interacting partner and AKT in PIK3CA cells. (A) Confocal immunofluorescence images of subcellular localization of cortactin (red) and pAKT (green) in MCF10A, Ex9-KI and Ex20-KI cells. Nuclei stained with DAPI. White arrows indicate the co-localization of cortactin and pAKT at peripheral

region of lamellipodia. Scale bar, 20 μm . Confocal immunofluorescence images of localization pattern of cortactin in red and cofilin (B), NCK1 (C) and WASP (D) in green in MCF10A, Ex9-KI and Ex20-KI cells. Nuclei were stained with 4,6-diamidino-2-phenylindole (DAPI). Scale bar = 20 μm .

Figure 4. Phosphorylation of cortactin in cancer cell lines with *PIK3CA* mutations.

(A) Phosphoproteomic strategy to validate cortactin phosphorylation sites in DLD1-wt, DLD1-mt and BT20 cells. (B) The panel shows a representative Coomassie blue stained gel from cortactin IP from BT20 cells. (C) Relative phosphorylation levels of cortactin in DLD1-wt and DLD1-mt cells, and (D) in BT20 cells treated with or without J124 or AKT inhibitor IV.

Figure 5. Cortactin is important in conferring migration/invasion ability in cells with *PIK3CA* mutations.

(A) Top panel: western blotting with cortactin antibody to assess the knockdown efficiency of siRNA targeting cortactin in MCF10A, Ex9-KI and Ex20-KI cells. β -Actin serves as loading control. Bottom panel: matrigel-coated Boyden chamber assays for the assessment of the migration/invasion ability of cells with indicated siRNA knockdown. (B,C) siRNA knockdown of cortactin in DLD1-mt (B) and BT20 cells (C). Top panels: western blotting of cortactin and b-actin; bottom panels: Boyden chamber assays of indicated cell lines.

Figure 6. AKT1-mediated phosphorylation on cortactin is important for migration/invasion induced by activation of PI3K.

(A) Top panel: Alignment of mRNA sequences of three cortactin isoforms. Red bar: mRNA segments, thin black line:

gaps, yellow arrow bars: CDS and short green arrows RT-PCR primers. Middle panel: Number of ESTs specifically matched to the alternative splicing sties. Bottom panel: RT-PCR results from MCF10A and Ex9-KI cells. Top panel: RT-PCR results from the upstream pair of primers differentiating isoform A and isoform B and/or C; middle panel: the downstream pair of primers differentiating isoform A and/or B and isoform C. Bottom panel: GAPDH as internal control. (B) Migration/invasion assays for MCF10A, Ex9-KI, Ex20-KI and (C) BT20 cells overexpressing wild-type cortactin isoform A and B (cortactin-wt) and phosphosite-mutated cortactin isoform A and B (cortactin-mut). Top panels: western blottings of overexpressed cortactin; bottom panels: migration/invasion assays of indicated cells. (D) Migration/invasion assays for MCF10A, Ex9-KI and Ex20-KI cells overexpressing wild type cortactin (cortactin-wt) treated with vehicle or AKT inhibitor (AKTi). The empty vector retrovirus infected cells served as controls. (B-D) Data are shown as mean±s.e.m. Mann–Whitney test was carried out to determine the statistical significance. These experiments were repeated at least twice.

Figure 7. A proposed model of enhancing invasiveness by oncogenic activation of PI3K-AKT signaling cascades and phosphorylation of cortactin. Cartoon depicts the proposed model of PI3K-AKT activation and phosphorylation of cortactin at four phosphorylation sites that leads to migration and invasion of cells.

Figure 1

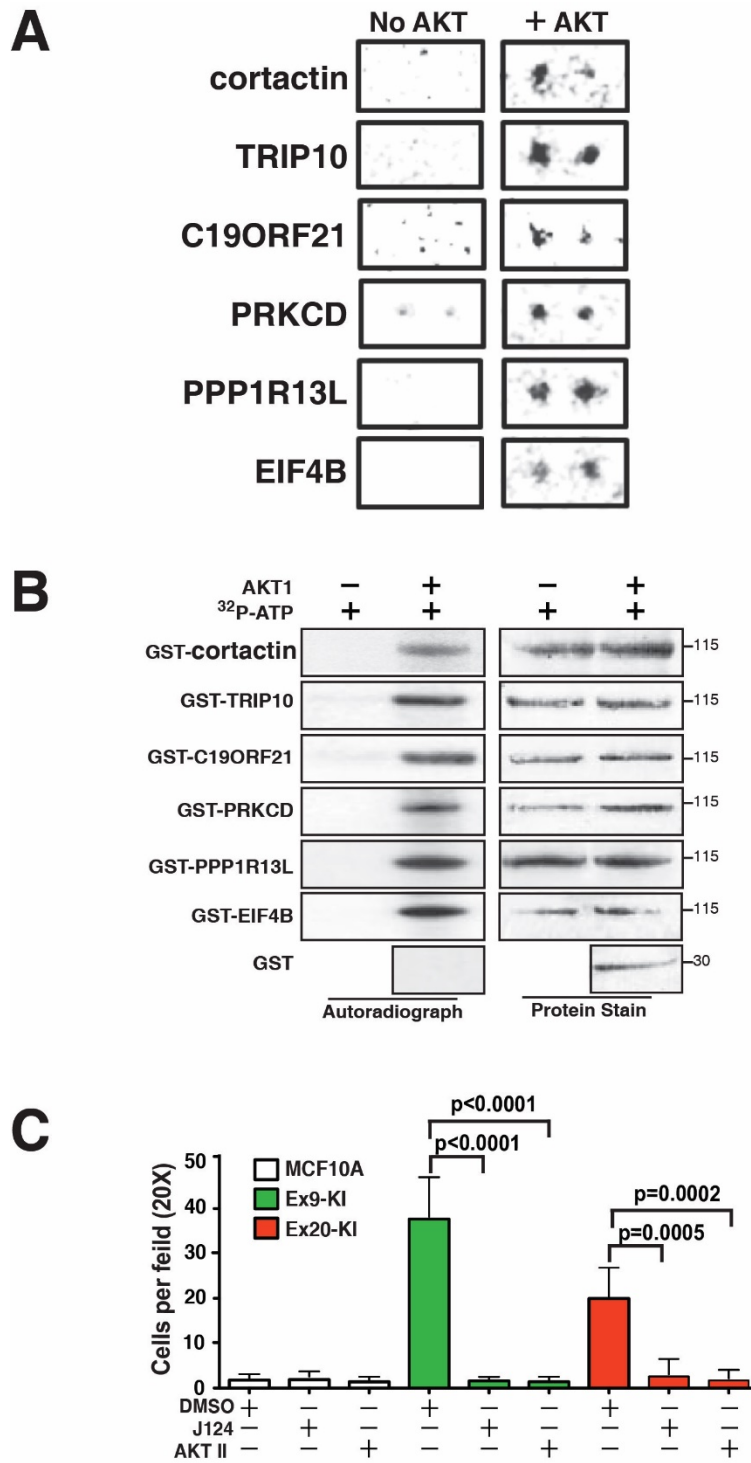


Figure 2

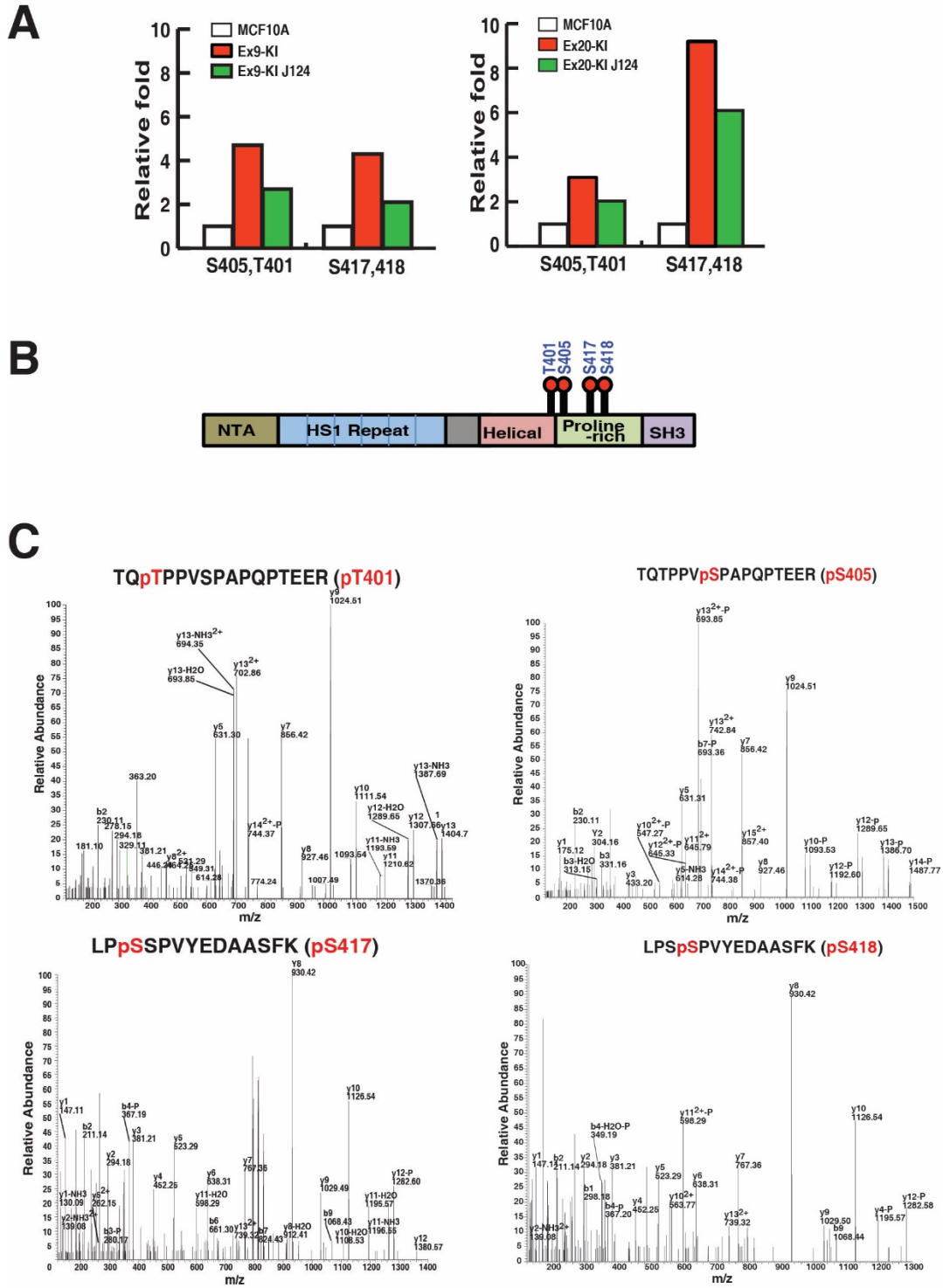


Figure 3

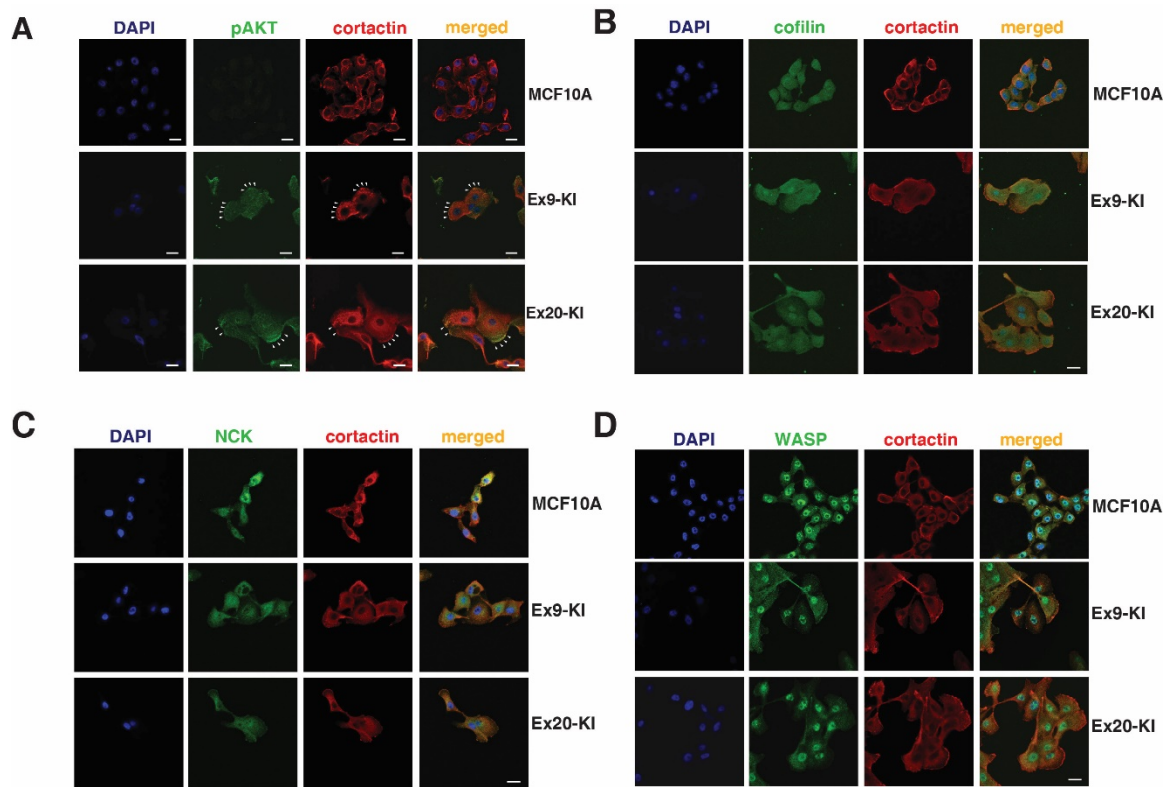


Figure 4

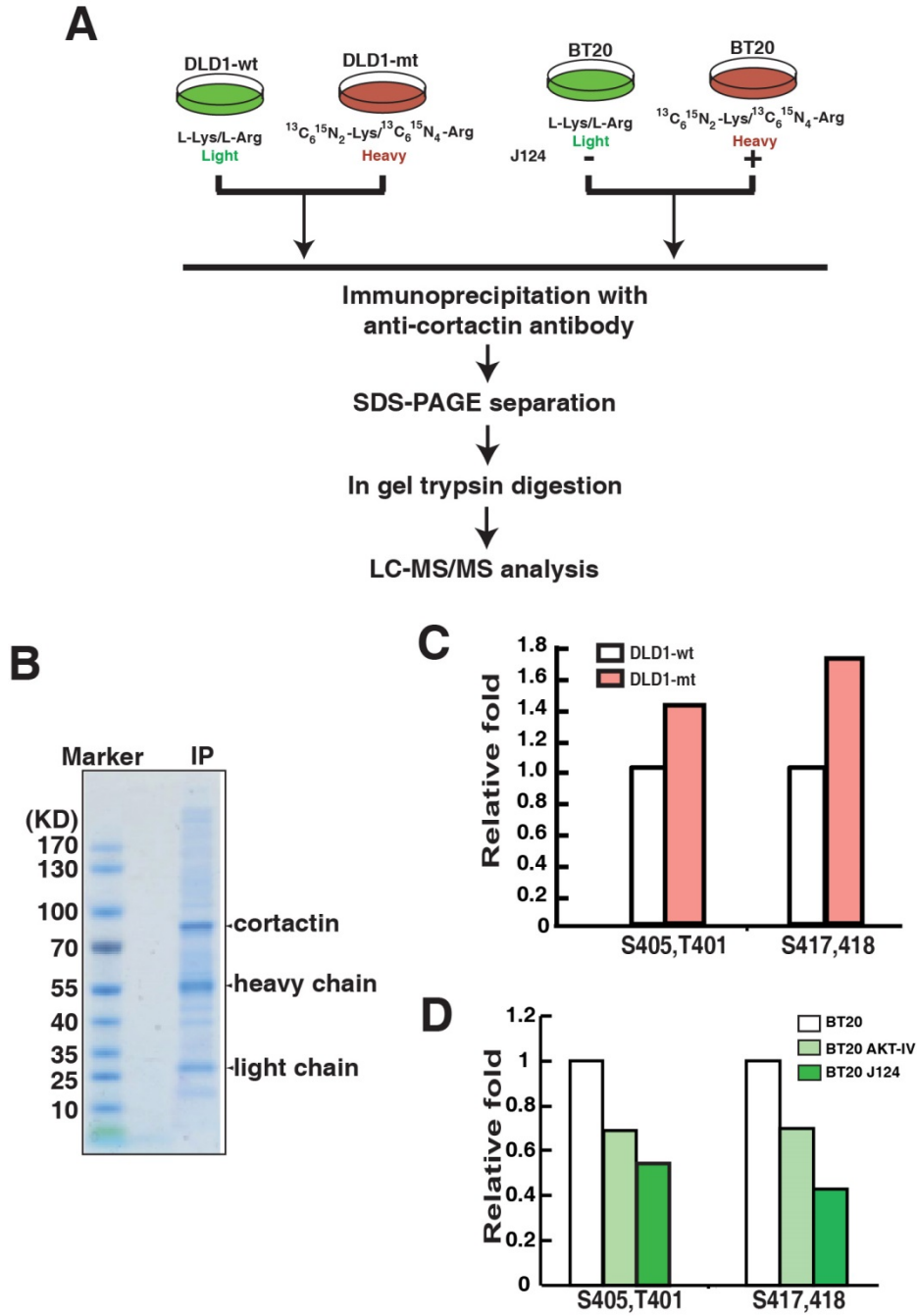


Figure 5

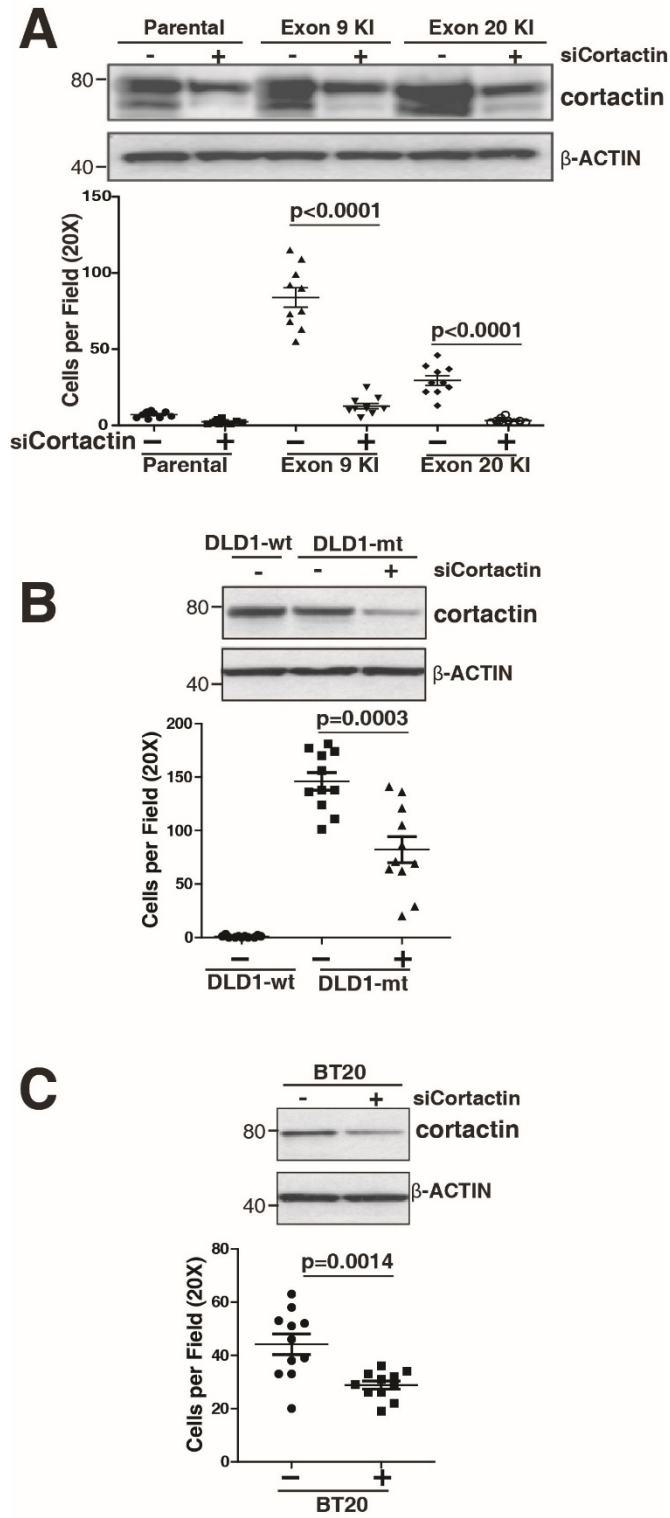


Figure 6

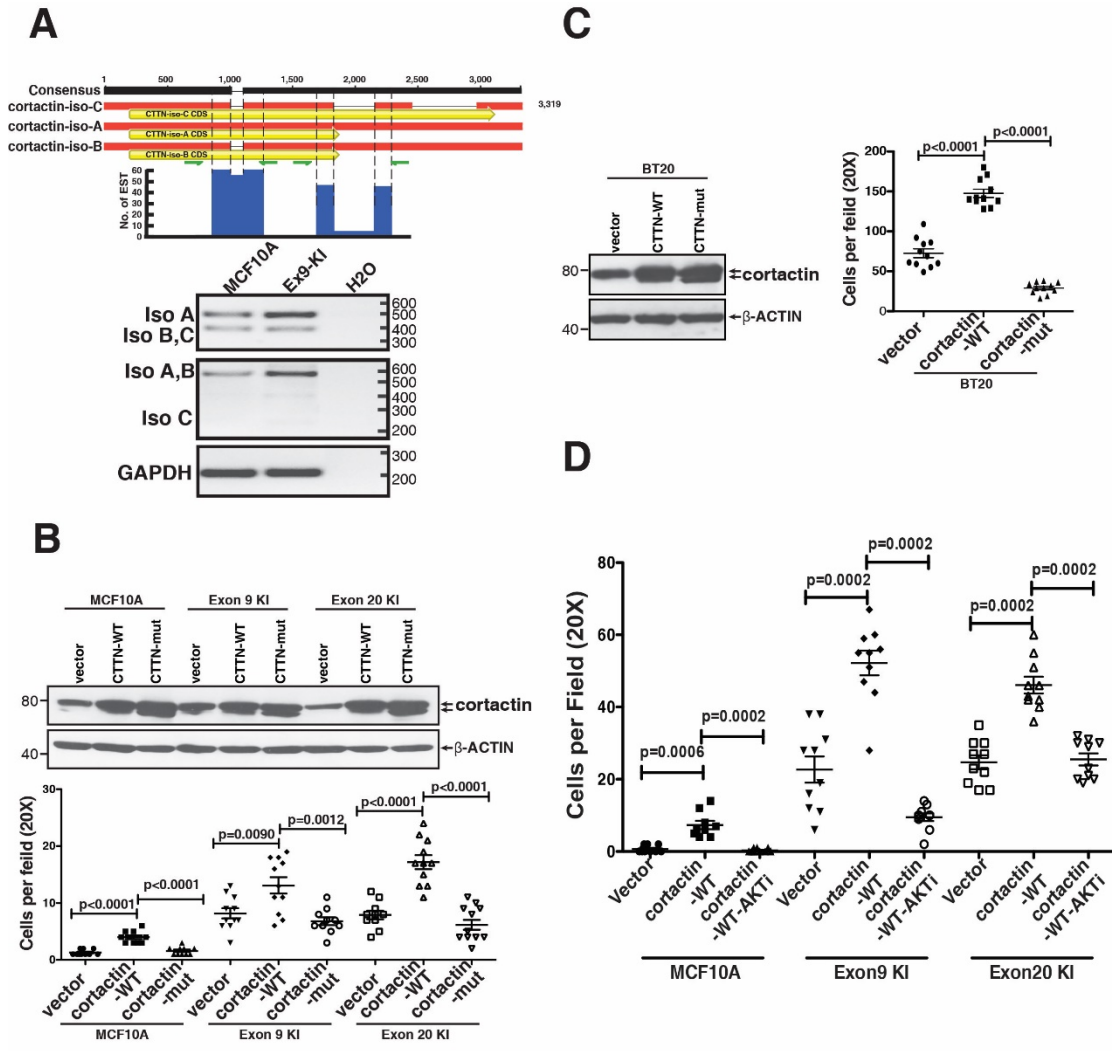
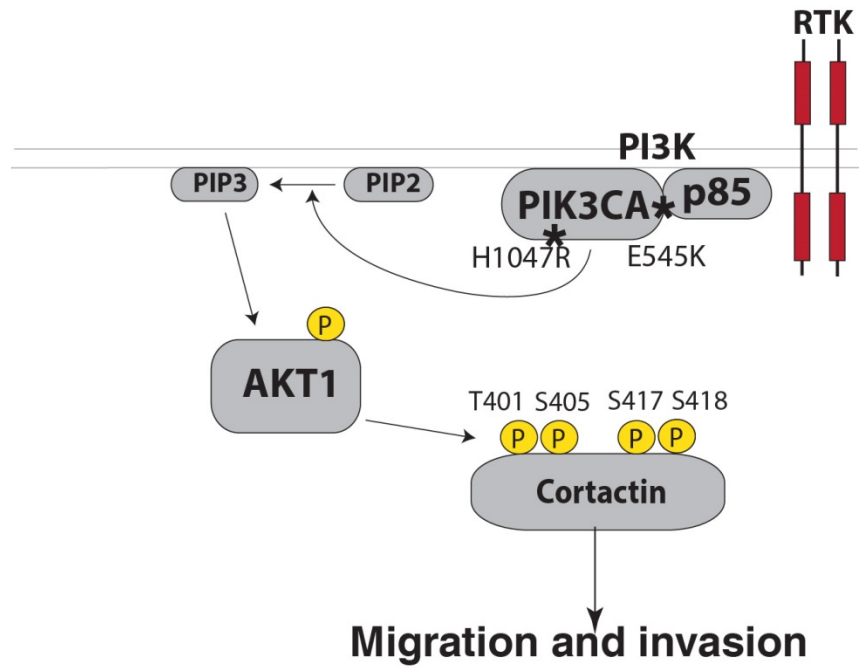


Figure 7



Chapter 4: Widespread modulation of the tyrosine phosphoproteome by *PIK3CA* mutations

Introduction

A majority of phosphorylation events in cells occur on serine and threonine residues of proteins with a very small fraction occurring on tyrosine residues. Even though tyrosine phosphorylation accounts for a minority of total phosphorylation, tyrosine kinases play a disproportionately large role in diseases especially in cancer. More than half of the 90 tyrosine kinases identified in the human proteome have been implicated in cancer through gain-of-function mutations, gene amplification, or overexpression, and have become attractive therapeutic targets. We have previously profiled the serine/threonine phosphoproteome of cells containing two hotspot mutations in *PIK3CA*, E545K and H1047R (Wu et al., 2014). In the current study, we sought to profile the tyrosine phosphoproteome changes that result from these activating mutations in *PIK3CA*. We performed phosphotyrosine profiling of these isogenic cell lines, where we identified 824 phosphopeptides derived from 343 proteins. We observed modulation of important biological processes that include cytoskeletal migration pathways and kinase regulated signaling. 127 of the identified phosphopeptides belong to 34 tyrosine kinases with 29 of these showing upregulation or downregulation of phosphorylation levels in the mutant knockin cell lines. This widespread modulation of tyrosine kinome indicates that there is a high degree of cross-talk between tyrosine kinase and serine/threonine kinase signaling pathways resulting from activation of the PI3K-AKT pathway.

Experimental procedures

Reagents

Anti-phosphotyrosine mouse mAb (pTyr-1000) beads were purchased from Cell Signaling Technology (Danvers, MA). TPKK-treated trypsin was obtained from Worthington Biochemical Corp. (Lakewood, NJ). DMEM/F12 with and without Lysine and Arginine, fetal bovine serum (FBS), L-glutamine, and antibiotics were purchased from Invitrogen (Carlsbad, CA). SILAC amino acids, $^{13}\text{C}_6$ -lysine, $^{13}\text{C}_6$ -arginine, $^2\text{H}_4$ -lysine, $^{13}\text{C}_6$ -arginine, $^{13}\text{C}_6^{15}\text{N}_2$ -lysine and $^{13}\text{C}_6^{15}\text{N}_4$ -arginine were purchased from Cambridge Isotope Laboratories (Andover, MA). All other reagents used in this study were from Fisher Scientific (Pittsburgh, PA).

Cell culture

PIK3CA mutant knock-in breast epithelial cell lines MCF10A (hereafter referred to as Ex9-KI and Ex20-KI) were established as previously described (Gustin et al., 2009). For experiments here, Ex9-KI cells, Ex20-KI cells, and MCF10A parental breast epithelial cells were cultured following a protocol similar to that previously described (Wu et al., 2014). All three cell lines (Ex9-KI, Ex20-KI and MCF10A) were grown in 5% CO_2 at 37 °C. Cell culture media consisted of DMEM/F12 (1:1) supplemented with 5% horse serum, 10 $\mu\text{g}/\text{ml}$ insulin (Roche), 0.5 $\mu\text{g}/\text{ml}$ hydrocortisone (Sigma), and 100 ng/ml cholera toxin (Sigma), and either 20 ng/ml EGF (for MCF10A parental cells) or 0.2 ng/ml EGF (for Ex9-KI and Ex20-KI cells).

Cell line labeling

Three-state stable isotopic labeling by amino acids in cell culture (SILAC) of MCF10A parental cells, Ex9-KI and Ex20-KI cells was performed. Briefly, cells were cultured in DMEM/F12 (1:1) SILAC media deficient in both L-lysine and L-arginine (Thermo Fisher Scientific). Ex20-KI cell culture media was supplemented with light lysine (K) and light arginine (R) to facilitate incorporation of the “light” labels. Ex9-KI cell culture media was supplemented with $^2\text{H}_4\text{-K}$ and $^{13}\text{C}_6\text{-R}$ to facilitate incorporation of the “medium” labels. Parental MCF10A cell culture media was supplemented with $^{13}\text{C}_6\text{-}^{15}\text{N}_2\text{-K}$ and $^{13}\text{C}_6\text{-}^{15}\text{N}_4\text{-R}$ to facilitate “heavy” state labeling. Prior to harvest, all cell lines were trypsinized, washed and seeded at 80% confluency in DMEM/F12 basal media containing only 5% horse serum and grown overnight. Two sets of three-state SILAC labeled cells were prepared as replicates for downstream mass spectrometry analysis.

In-solution trypsin digestion

Following cell culture, peptides were prepared in an in-solution tryptic digestion protocol with slight modifications (Rush et al., 2005). Briefly, cells were lysed in urea lysis buffer (20 mM HEPES pH 8.0, 9 M urea, 1 mM sodium orthovanadate, 2.5 mM sodium pyrophosphate, 1 mM β -glycerophosphate and 5mM sodium fluoride), sonicated and then cleared by centrifugation at $15,000 \times g$ at 4°C for 20 minutes. As determined by BCA assay, 20 mg protein from each SILAC-labeled cell lysate was mixed. The resultant mixture was then reduced with 5 mM dithiothreitol and alkylated with 10 mM

iodoacetamide. For in-solution tryptic digestion, the resulting protein extracts were diluted in 20 mM HEPES pH 8.0 to a final concentration lower than 2 M urea incubated with 1 mg/mL TPCK-treated trypsin on an orbital shaker at 25°C overnight. Protein digests were acidified with 1% trifluoroacetic acid (TFA) to quench the digestion reaction and then subjected to centrifugation at 2,000 x g at room temperature for 5 min. The resulting supernatants were desalted using SepPak C₁₈ cartridge. Eluted peptides were lyophilized to dryness prior to phosphotyrosine peptide enrichment.

Basic reversed-phase liquid chromatography (RPLC)

For the total proteome analysis, basic RPLC was carried out as previously described (Wang et al., 2011). Agilent 1100 offline LC system was used for bRPLC fractionation which includes a binary pump, VWD detector and an automatic fraction collector. Briefly, lyophilized samples were reconstituted in solvent A (10 mM triethylammonium bicarbonate, pH 8.5) and loaded onto XBridge C₁₈, 5 µm 250 × 4.6 mm column (Waters Corporation, Milford, MA, USA). Peptides were resolved using a gradient of 3 to 50 % solvent B (10 mM triethylammonium bicarbonate in acetonitrile, pH 8.5) over 50 min and then kept at 90% for another 10 minutes. A total of 96 fractions were collected and these were concatenated into 12 fractions. Samples were then dried in vacuum and stored in -80°C freezer prior to LC-MS/MS analysis.

Immunoaffinity purification of phosphotyrosine peptides

Immunoaffinity purification (IAP) of phosphotyrosine peptides was performed as previously described (Rush et al., 2005). Briefly, following lyophilization, desalted lyophilized tryptic peptide were reconstituted in 1.4 mL of IAP buffer (50mM MOPS pH 7.2, 10mM sodium phosphate, 50mM NaCl) and subjected to centrifugation at 2,000 x g at room temperature for 5 min. Prior to IAP, anti-phosphotyrosine antibody beads (pY1000, Cell Signaling Technology) were washed with IAP buffer once. The reconstituted peptide mixtures were then incubated with anti-phosphotyrosine antibody beads on a rotator at 4°C for 30 minutes. Samples were then centrifuged at 1,500 x g for 1 minute and supernatant was removed. The beads were washed twice with IAP buffer and then twice with water. Residual water was removed. Phosphopeptides were eluted from the antibody beads by acidifying the bead mixture at room temperature with 0.1% TFA. Phosphopeptides eluents were desalted with C18 STAGE tips, vacuum dried and stored at -80°C prior to LC-MS/MS analysis.

Liquid chromatography tandem mass spectrometry

Data dependent LC-MS/MS analysis of phosphopeptides enriched by IAP was performed with an LTQ-Orbitrap Elite mass spectrometer (Thermo Fisher Scientific) coupled to a nano-liquid chromatography system (Proxeon, Easy Nano-LC). During each LC-MS/MS run, 10 uL of reconstituted peptide solution were injected onto a nano-c18 reversed phase column (10 cm × 75 µm, Magic C18 AQ 5 µm, 120 Å). Peptides were then fractionated across a 90-minute linear reversed phase HPLC gradient (from 5 to 60% Acetonitrile). High-resolution precursor scans (FTMS) were acquired within the Orbitrap analyzer across a mass range of 350-1,700 Daltons (with 120,000 resolution at 400 m/z). The

fifteen most abundant precursor ions from each precursor scan were selected for High Collision Dissociation (HCD) fragmentation (isolation width of 1.90 m/z; 32% normalized collision energy and activation time of 0.1ms). High-resolution MS/MS spectra were acquired (at 30,000 resolution at 400 m/z) on the Orbitrap analyzer following fragmentation.

Mass spectrometry data analysis

The Proteome Discoverer (v 1.4; Thermo Fisher Scientific) software package was used to facilitate downstream protein identification and quantitation. All acquired mass spectrometric data were searched within the Proteome Discoverer interface using both Mascot (Version 2.2.0) and SEQUEST search algorithms against Human RefSeq database v 50 (containing 35,478 entries). For both algorithms, search parameters were as follows: a maximum of two missed cleavages; a fixed modification of carbamidomethylation; variable modifications of N-terminal acetylation, oxidation at methionine, phosphorylation at serine, threonine and tyrosine and SILAC labeling $^{13}\text{C}_6$, $^{15}\text{N}_2$ -lysine; $^2\text{H}_4$ -lysine; $^{13}\text{C}_6$ -arginine and $^{13}\text{C}_6$, $^{15}\text{N}_2$ -arginine; MS tolerance of +/-10 ppm; MS/MS tolerance of +/-0.1 Da. The Mascot and SEQUEST score cut-offs were set to a false discovery rate of 1% at the peptide level. The q values for the peptides were calculated using the Percolator algorithm within the Proteome Discover suite. The peptide quantification was performed using the algorithms available within the precursor ion quantifier node. Quantitation was determined based on area under the curve measurements from the extracted ion chromatograms for each precursor ion. The probability that an identified phosphorylation was modifying each specific Ser/Thr/Tyr

residue on each identified phosphopeptide was determined from the PhosphoRS algorithm (Taus et al., 2011). We averaged and normalized the intensities of the phosphopeptides identified in the two replicate experiments that were carried out. Total sum intensities of all phosphopeptides for each SILAC label were used to normalize the phosphopeptide abundance. 1.5-fold cut-off was selected for hyperphosphorylation and a 0.67-fold cut-off was selected to denote hypophosphorylation. All mass spectrometry proteomics data associated with this project have been deposited to the ProteomeXchange Consortium (<http://proteomecentral.proteomexchange.org>) via the PRIDE partner repository with the dataset identifier PXD001460.

Western blot analysis

All cell lines used for western blot analyses were cultured in regular medium with light amino acids. Prior to harvest, cells were seeded overnight in medium containing only 5% horse serum. Cells were harvested and lysed in modified RIPA buffer (50 mM Tris-HCl, pH 7.4, 150 mM NaCl, 1 mM EDTA, 1% Nonidet P-40, 0.25% sodium deoxycholate, and 1 mM sodium orthovanadate in the presence of protease inhibitors). Whole cell protein extracts were denatured and separated in NuPAGE gels (Invitrogen), transferred to nitrocellulose membranes, and probed with primary and horseradish peroxidase-conjugated secondary antibodies. The primary antibodies used were anti-phospho-EGFR Y1173 (4407; Cell Signaling Technology), anti-EGFR (2232; Cell Signaling Technology), anti-phospho-EPHA2 Y588 (12677; Cell Signaling Technology), anti-EPHA2 (6997; Cell Signaling Technology), anti-phospho-MET Y1003 (3135; Cell Signaling Technology), anti-MET (3148; Cell Signaling Technology), anti-phospho-

EFNB1 Y324 (OAAF00520; Aviva Systems Biology), anti-EFNB1 (ARP46450_P050; Aviva Systems Biology) phospho-HER2 Y877 (2265-1; Epitomics), anti-HER2 (2165; Cell Signaling Technology), and anti- β -ACTIN (A5316, Sigma).

Results

Phosphotyrosine profiling of mutant PIK3CA knockin cells reveals widespread modulation of the tyrosine phosphoproteome

The p110 α subunit of PI3K is composed of an N-terminal p85 binding domain, a Ras binding domain, a C2 domain, a helical domain and a kinase domain (Figure 1A) (Amzel et al., 2008). The gene encoding p110 α , *PIK3CA*, has been shown to be frequently mutated in human cancers (Samuels et al., 2004). The cBioPortal for Cancer Genomics online tool (www.cbioportal.org), which compiles sequencing data from large scale sequencing studies of human cancers, revealed three hotspot mutations in this gene (Figure 1a) (Cerami et al., 2012; Gao et al., 2013). Two of these mutations occur in exon 9 of the gene (E542K and E545K), which codes for the helical domain, and another mutation occurs in exon 20 of the gene (H1047R), which codes for the kinase domain. These single amino acid mutations result in a gain of function of PI3K, which ultimately leads to activation of AKT signaling and inducing growth-factor and anchorage-independent growth, cell motility and tumor formation *in vivo* (Ikenoue et al., 2005; Kang et al., 2005; Zhao et al., 2005). We previously established cell lines that contain the E545K and H1047R mutations (hereafter referred to as Ex9-KI and Ex20-KI, respectively) using gene targeting to knock in these mutations into the spontaneously

immortalized, non-tumorigenic breast epithelial cell line MCF10A (Gustin et al., 2009). A breast epithelial cell line model is especially relevant as *PIK3CA* has been shown to be the most frequently mutated gene across all subtypes of breast tumors (Bachman et al., 2004; Network, 2012). In a previous study, we have carried out phosphoserine/threonine profiling of these isogenic cell lines using TiO₂ phosphopeptide enrichment (Wu et al., 2014). We found multiple receptor and non-receptor tyrosine kinases including EGFR, EPHA2 and PTK2 to be hyperphosphorylated in the mutant cells, which led us to hypothesize that tyrosine kinases, and subsequently their downstream signaling pathways, are activated in *PIK3CA* mutant cells. In the current study, we aimed to perform an in-depth analysis of tyrosine kinase signaling pathways by specifically enriching for tyrosine phosphorylated peptides. To this end, we performed SILAC (stable isotope labeling by amino acids in cell culture) labeling on the mutant knock-in cell lines along with the parental MCF10A to allow for accurate quantitation of phosphorylation levels. The three state-SILAC experiment was carried out by mixing equal amounts of protein lysates from Ex20-KI cells labeled with light SILAC medium, Ex9-KI (medium) and parental MCF10A (heavy). The mixture was digested with trypsin and the tryptic peptides were then desalted using the C₁₈ cartridge. Phosphotyrosine enrichment of the phosphopeptides was carried out using the anti-phosphotyrosine antibody pulldown prior to LC-MS/MS analysis (Figure 1B).

From this profiling, we identified 824 phosphopeptides from 343 proteins. A majority of these phosphopeptides (651) are phosphorylated on tyrosine residues, and a smaller fraction on serine/threonine residues (173). Most of these phosphopeptides showed similar phosphorylation pattern in both Exon 9 and Exon 20 (Figure 2A). We

observed a global elevation of protein phosphorylation level in the mutant knock-in compared to the parental cells, where more peptides showed upregulation in phosphorylation levels compared to downregulation (Figure 2B). This indicates that *PIK3CA* mutations lead to a global increase in protein phosphorylation levels and hence profoundly impact the tyrosine signaling pathways. In order to investigate the stoichiometry of the observed phosphorylation-site changes, we performed a global proteome analysis of the same cell lines. We observed that most of the proteome did not change in the knock-in cell lines, indicating that tyrosine phosphoproteome modulation is mostly due to the activation of tyrosine kinases (Figure 2D). In our previous work⁴, we identified 166 phosphotyrosine-containing peptides out of 8,075 phosphopeptides identified. In the current study, we identified 651 phosphotyrosine-containing peptides out of 824 phosphopeptides identified, a number four times larger than our previous study. More importantly, none of the phosphotyrosine-containing peptides identified in our previous study belong to any of the tyrosine kinases in the human proteome (11 tyrosine kinases were identified from phosphoserine/threonine-containing peptides), whereas our current study identified 34 tyrosine kinases with 29 of these showing alterations in their phosphorylation status. This indicates the necessity of phosphotyrosine peptide-specific enrichment in order to study the tyrosine phosphoproteome modulation in the cells.

Analysis using KEGG pathway database showed that many of these hyperphosphorylated proteins are involved in important biological processes such as cell motility, which includes pathways in regulation of actin cytoskeleton, focal adhesion, tight and adherens junctions, as well as kinase regulated pathways such as ErbB, insulin

and VEGF signaling pathways (Figure 2C). Of particular note, many of these pathways were also found to be regulated through our phosphoserine/threonine profiling in our previous study, supporting the robustness of our mass spectrometry analysis (Wu et al., 2014). Activation of these pathways in the *PIK3CA* mutant cells could potentially explain why these cells are able to proliferate in the absence of growth factors and are significantly more invasive than the wild type cells.

Activating PIK3CA mutations modulate the tyrosine kinome

Of the 343 proteins that we identified from our profiling, 63 are protein kinases. 34 of these belong to the tyrosine kinase family where 16 are receptor tyrosine kinases and 18 are non-receptor tyrosine kinases. We mapped the identified kinases onto the phylogenetic tree of the human kinome (Figure 3). A majority of the phosphopeptides from these kinases showed either an increase or decrease in phosphorylation levels, suggesting that the activity of these kinases is regulated. This regulation signifies that the signaling pathways downstream of these kinases, for example the focal adhesion pathway and ErbB signaling pathway (Figure 2C), are also modulated. More kinases were found to have increased levels of phosphorylation compared to decreased levels of phosphorylation. Figure 4 shows representative spectra of phosphopeptides belonging to these kinases. As shown in this figure, Ex9-KI and Ex20-KI cells have increased phosphorylation compared to the parental MCF10A cells. Many of the identified sites on these hyperphosphorylated kinases have been implicated in oncogenic transformation or metastasis. For instance, phosphorylation of EGFR at Y1110 has been reported to stimulate cancer cell invasion, motility and migration (Cardoso et al., 2014).

Phosphorylation of Y588 of EPHA2 has been reported to be critical for vascular assembly and tumor angiogenesis (Fang et al., 2008). Thus the phosphorylation of these kinases could contribute to the oncogenic effects that are observed in cells with *PIK3CA* mutation.

One possible mechanism of how these kinases were activated is through direct phosphorylation by AKT. Both EGFR and EPHA2 have been demonstrated to be substrates of AKT. EGFR S229 phosphorylation by AKT was shown to contribute to drug resistance and EPHA2 S897 phosphorylation by AKT was found to stimulate cell migration (Huang et al., 2011; Miao et al., 2009). AKT phosphorylation on these sites could lead to phosphorylation of other tyrosine residues on EGFR and EPHA2 through autophosphorylation and dimerization. The activated EGFR and EPHA2 could heterodimerize with other family members such as ERBB2 (Goldman et al., 1990; Wada et al., 1990), leading to the hyperphosphorylation of many members of epidermal growth factor receptor family and ephrin receptor family, which was observed in the *PIK3CA* mutant cells. Another possible mechanism of tyrosine kinase activation in the mutant cell is through direct activation by PIP₃. There are four tyrosine kinases which contain the pleckstrin homology domain that can bind to PIP₃, namely BMX, BTK, TEC and TIK. Studies have demonstrated that mutant *PIK3CA* could activate BMX, which could in turn directly phosphorylate STAT3 on Y705 (Guryanova et al., 2011; Hart et al., 2011). In our profiling, we found STAT3 Y705 to be hyperphosphorylated 2.3-fold in Ex9-KI and 1.6-fold in Ex20-KI cells, suggesting that this mechanism is also active in the mutant cells. However, the hyperphosphorylation of many of the tyrosine kinases we identified could not be explained simply by activation through PIP₃ or AKT pathway. Thus this indicates

that there are activations of various tyrosine kinase signaling through cross-talks and other mechanisms that are still not well-elucidated.

Site-specific analysis of tyrosine kinase phosphorylation regulated by PIK3CA mutations

To understand the effects of regulation of phosphorylation of the tyrosine kinases, we mapped the phosphorylation sites we identified in our profiling onto the protein structure. The receptor tyrosine kinases that exhibit regulation of phosphorylation levels are shown in Figure 5a and the non-receptor tyrosine kinases are depicted in Figure 5b. Receptor tyrosine kinases are composed of a large extracellular domain which binds to ligands, a transmembrane domain and a cytoplasmic tail which contains the tyrosine kinase domain. All of the phosphorylation sites we identified were localized on the cytoplasmic tail, indicating that regulation of activity occurs intracellularly. Non-receptor tyrosine kinases typically contain a tyrosine kinase domain along with other domains such as SH2 and SH3 which allow interaction and binding to other proteins. In both receptor and non-receptor tyrosine kinases, we observed that many of the regulated phosphorylation sites lie within the tyrosine kinase domain. The phosphorylation of many of the sites in this domain has been shown to be important for activity of the corresponding kinases. This includes Y877 of ERBB2, better known as HER2 (Adams, 2003; Bose et al., 2006; Huse and Kuriyan, 2002), Y869 of EGFR (Biscardi et al., 1999; Tice et al., 1999), Y772 of EPHA2 (Fang et al., 2008), Y1189 and Y1190 of INSR (Jacob et al., 2002), Y714 of FER (Hikri et al., 2009) and Y347 of TNK2 (Yokoyama and Miller, 2003, 2006), all of which were found to be hyperphosphorylated in the mutant cells. We also observed many known regulatory sites outside of the tyrosine kinase

domain to be hyperphosphorylated in the mutant cells. These include the C-terminal Y1197 autophosphorylation site of EGFR which has been reported to be important for its enzymatic activity in addition to serving as a docking site for substrates such as PLC- γ and Shc (Jorissen et al., 2003; Sorkin et al., 1991, 1992). Phosphorylation of the juxtamembrane region of EPHB2 has been demonstrated to stimulate its catalytic activity by removing the inhibitory conformation of this region and serving as recruitment sites for proteins containing SH2 domains such as Ras-GAP (Holland et al., 1997; Wybenga-Groot et al., 2001). Similarly, phosphorylation of Y323 of SYK has been reported to be required for the interaction with its substrate Cbl and the maximal tyrosine phosphorylation of Cbl (Deckert et al., 1998). Taken together, the preponderance of regulated sites identified in the kinase domain and regulatory regions signifies that these kinases and their downstream signaling pathways are activated. In addition to these well-studied sites, there are other sites which were found to be regulated in the mutant cells whose functions are still unknown. Determining the significance of these phosphorylation sites in inducing oncogenic effects downstream of PI3K will require additional studies.

Validation of the phosphoproteomic screen by western blot analysis

To validate our phosphoproteomic screen, we performed western blot analysis using antibodies against phosphorylated sites of proteins identified in our global profiling, namely EGFR, EPHA2, MET, EFNB1 and ERBB2. For each of these antibodies, we showed through western blot that the levels of phosphorylation are consistent with our mass spectrometry results (Figure 6). For example, we found EGFR Y1197 and EPHA2 Y588 to be hyperphosphorylated at about 2-fold in Ex9-KI and Ex20-

KI cells, and we observed a consistent increase in signal in our western blot. ERBB2 Y877 on the other hand only showed elevation in Ex20-KI (2-fold) but not in Ex9-KI (1.1-fold) and we confirmed this data with our western blot. MET Y1021 did not show marked elevation of phosphorylation in our profiling data in Ex9-KI (1.3-fold) and Ex20-KI (1.1-fold), which was supported by the western blot analysis. We also performed western blot of total protein for each of these proteins and we observed similar levels of protein expression in each of MCF10A parental, Ex9-KI and Ex20-KI cells (except for HER2 where we observed a slight decrease of protein levels in mutant cells even though the phosphorylation levels increased). This indicates that these proteins are hyperphosphorylated through activation of kinases and not as a result of transcriptional/translational regulation. Thus we have demonstrated through an orthogonal method that our mass spectrometry profiling data are accurate.

Discussion

Through phosphoproteomic profiling of cells with a single amino acid change in the *PIK3CA* gene, we demonstrate that there is a widespread modulation of the tyrosine phosphoproteome due to these activating mutations. Even though these mutations have been shown to result primarily in the hyperactivation of pathways downstream of the serine/threonine kinase AKT, our results clearly indicate that tyrosine signaling pathways are also widely affected. The activation of a few tyrosine kinases in the mutant *PIK3CA* cells could be the result of direct binding to PIP₃ or direct phosphorylation by AKT. However many others could not be explained through these mechanisms as phosphotyrosine signaling is generally not studied in the context of serine/threonine

kinases. This suggests that there are hitherto unknown mechanisms of crosstalk that occur between these pathways. Our profiling study should serve as a potentially useful resource for research as well as clinical studies involving development of novel therapeutic targets.

FIGURE LEGENDS

Figure 1. Phosphoproteomic analysis of MCF10A cells with PIK3CA mutations.

(A) Diagram of the p110 α subunit encoded by the *PIK3CA* gene with the frequency of mutations found in large scale human sequencing studies. p85: p85 binding domain; RBD: Ras binding domain. Modified from www.cbioportal.org. (B) A schematic depicting the strategy used for quantitative phosphoproteomic profiling of *PIK3CA* Ex9 and Ex20 knockin mutant cells.

Figure 2. Phosphotyrosine profiling results of MCF10A with PIK3CA mutations.

(A) Density scatter plot of log₂-transformed phosphopeptide ratios (Ex9-KI/MCF10A vs Ex20-KI/MCF10A). Pearson correlation coefficient (R) is indicated. (B) Distribution of log₂-transformed phosphopeptide ratios (Ex9-KI/MCF10A vs Ex20-KI/MCF10A). (C) The number of regulated proteins found in enriched signaling pathways (Modified Fisher's exact *P*-value <0.05).

Figure 3. Widespread modulation of the kinome by PIK3CA mutants.

Phylogenetic tree of protein kinases is denoted with kinases identified in phosphoproteomic profiling. A color-coded site regulation pattern is shown in the form of a circle divided into two parts. The top half represents the fold change of phosphorylation sites identified in Ex-9-KI cells and the bottom half represents Ex20-KI cells compared with MCF10A.

Figure 4. Hyperphosphorylation of tyrosine kinases in the PIK3CA mutant cells.

Representative MS spectra of tyrosine phosphopeptides belonging to EPHB4, EGFR,

ABL1 and EPHA2 tyrosine kinases showing higher levels in the Ex9-KI and Ex20-KI cells compared to the parental MCF10A cells.

Figure 5. Site-specific regulation of tyrosine kinases by *PIK3CA* mutations. Diagram representations of receptor tyrosine kinases (A) and non-receptor tyrosine kinase (B) denoted with phosphorylation sites found to be regulated in either Ex9-KI (top half of circle) or Ex20-KI (bottom half of circle).

Figure 6. Validation of phosphoproteomic results. Western blot analysis using phospho-specific antibodies against EGFR, EPHA2, MET, EFNB1, and ERBB2 and the corresponding total protein antibodies. β -actin serves as a loading control.

Figure 1

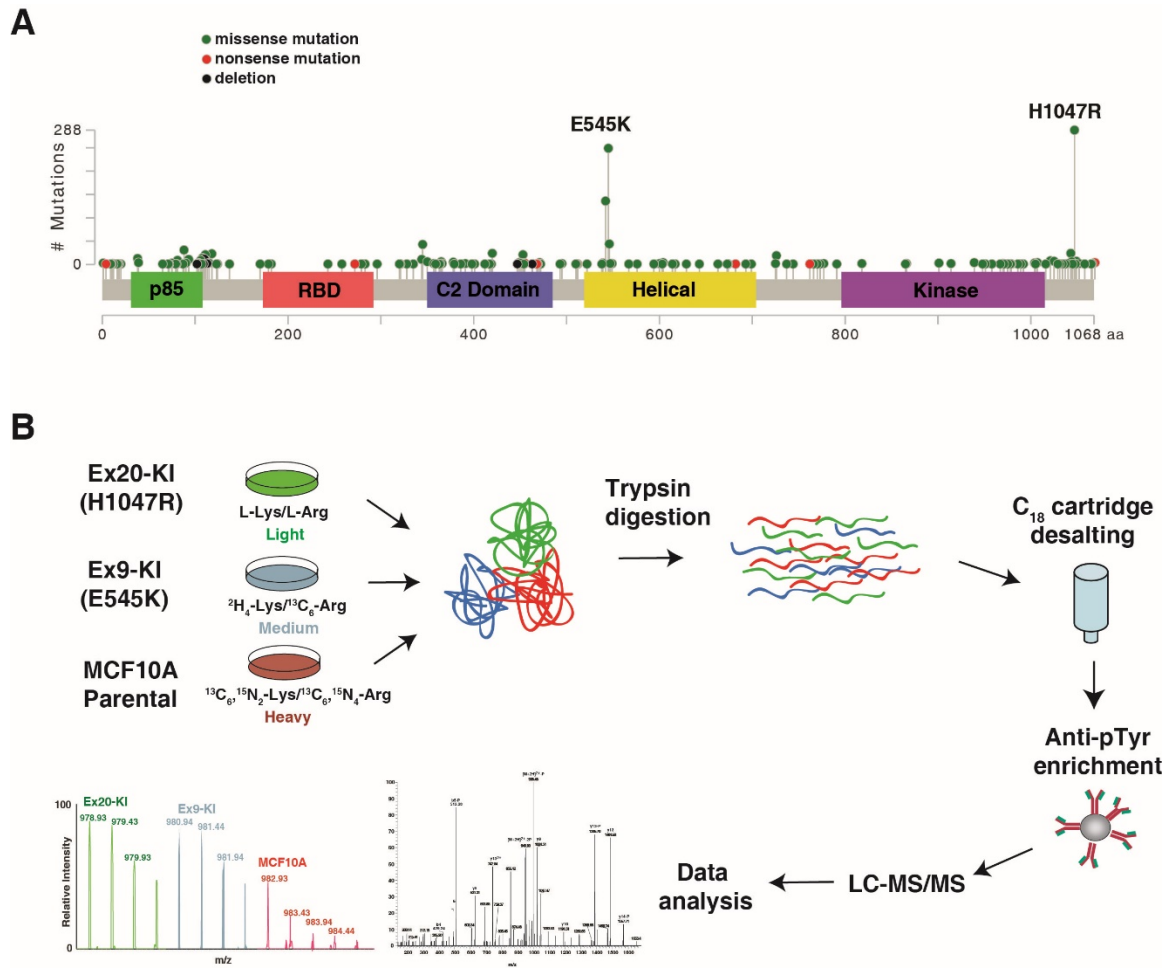


Figure 2

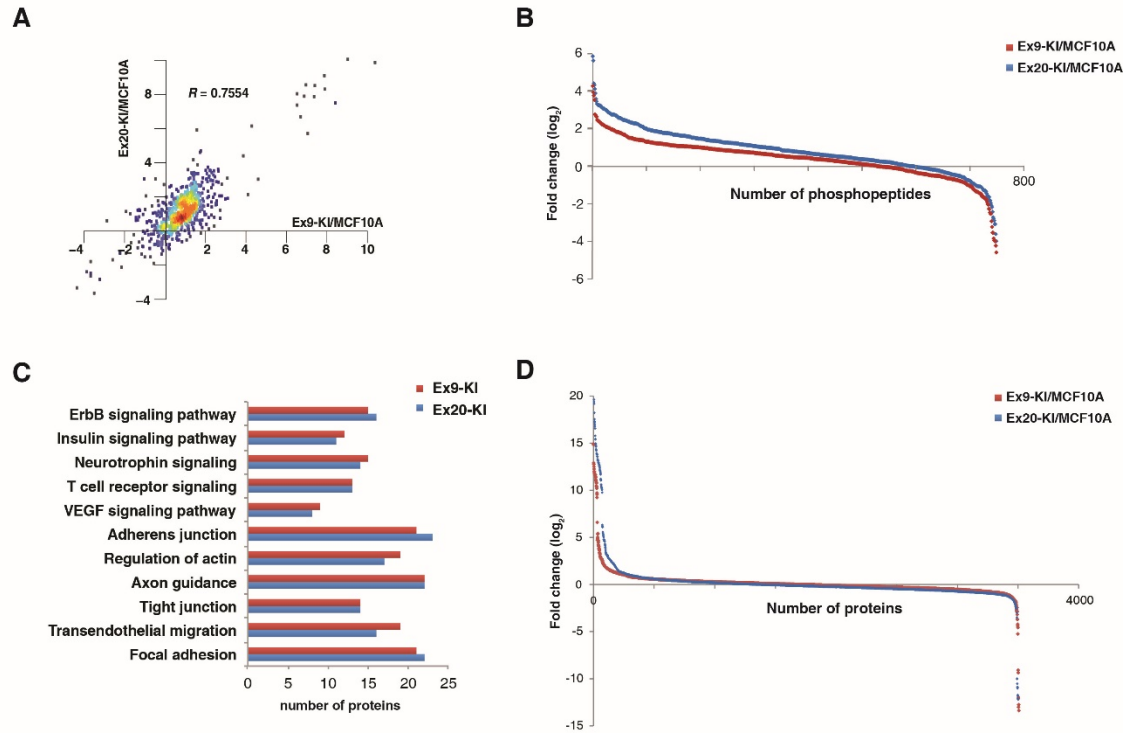


Figure 3

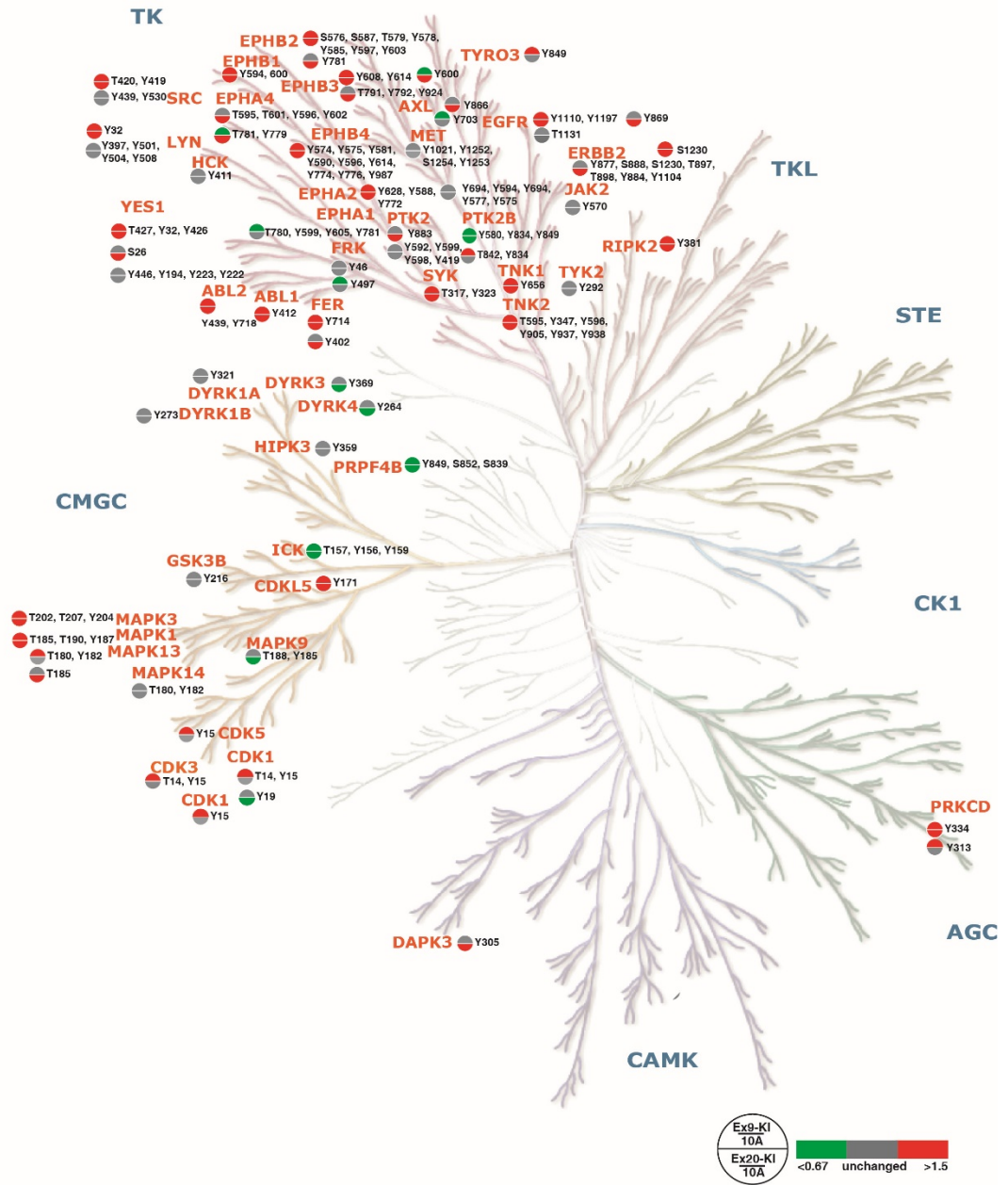


Figure 4

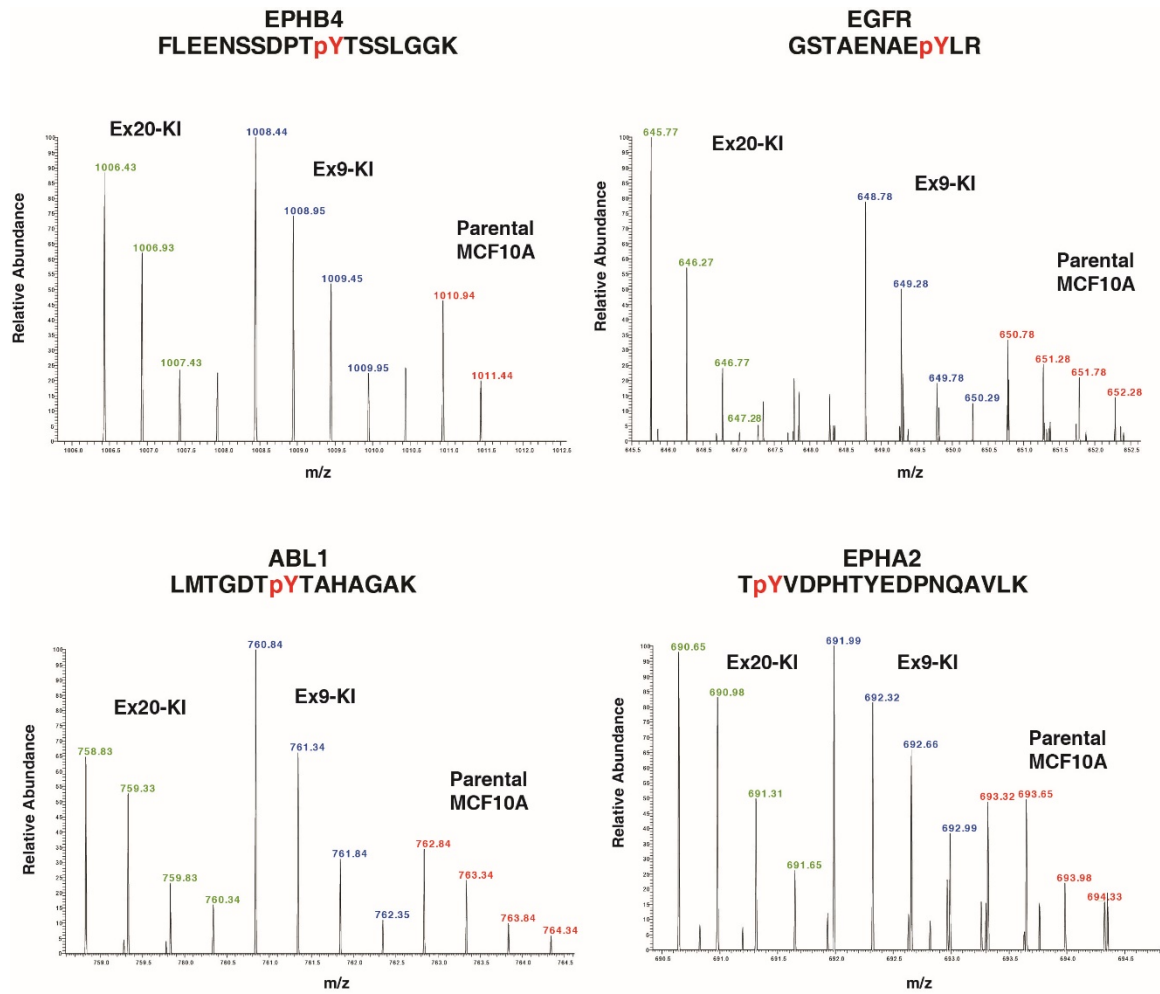


Figure 5

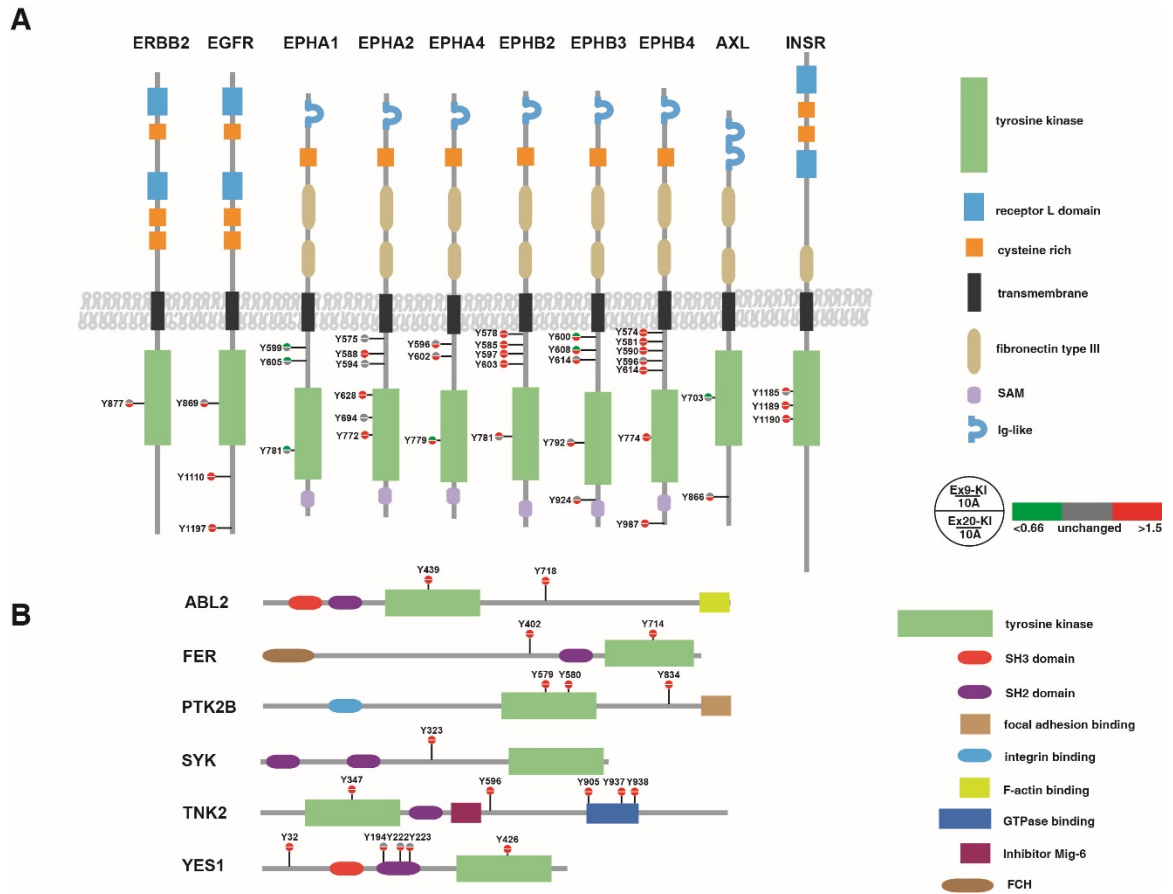
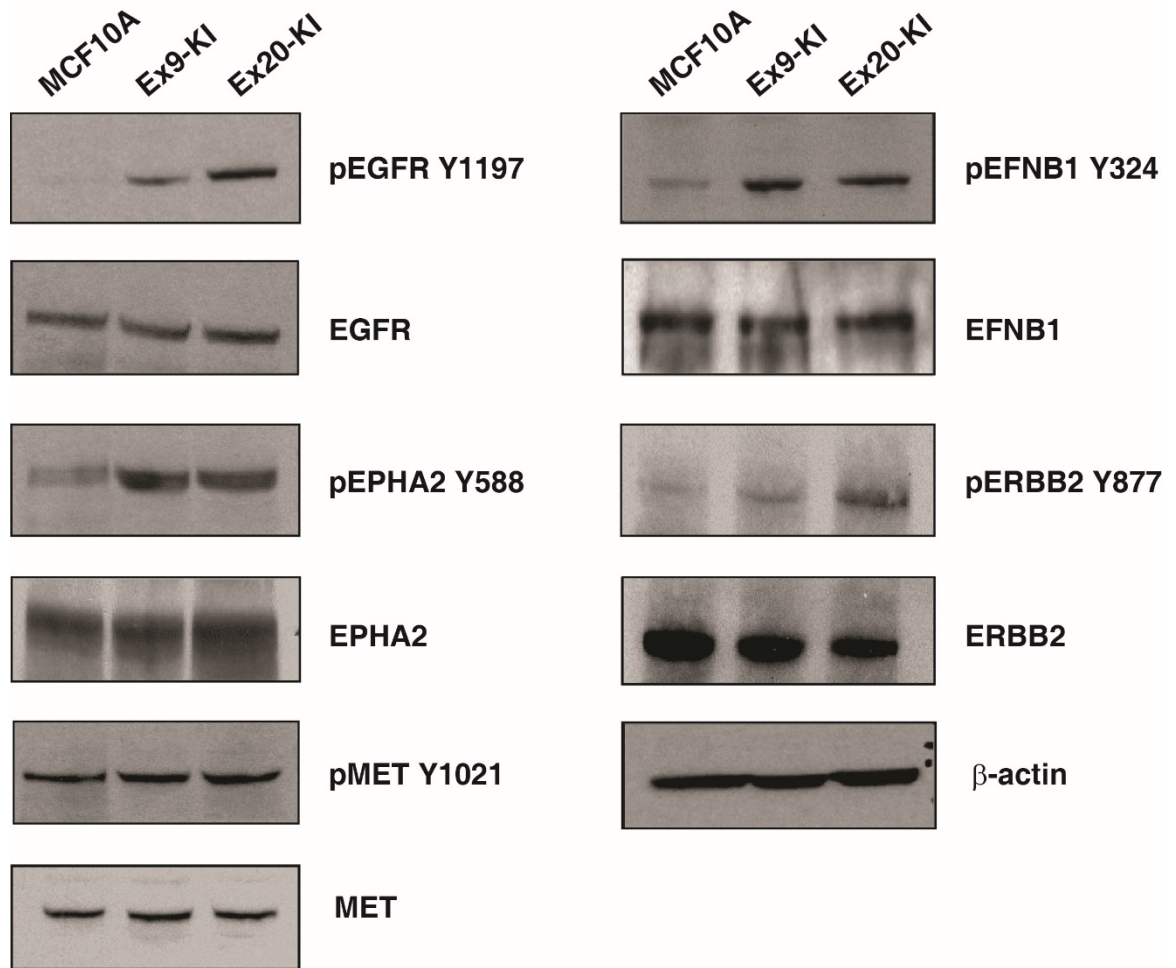


Figure 6



Chapter 4: References

Adams, J.A. (2003). Activation Loop Phosphorylation and Catalysis in Protein Kinases: Is There Functional Evidence for the Autoinhibitor Model?†. *Biochemistry (Mosc.)* 42, 601–607.

Amzel, L.M., Huang, C.-H., Mandelker, D., Lengauer, C., Gabelli, S.B., and Vogelstein, B. (2008). Structural comparisons of class I phosphoinositide 3-kinases. *Nat. Rev. Cancer* 8, 665–669.

Bachman, K.E., Argani, P., Samuels, Y., Silliman, N., Ptak, J., Szabo, S., Konishi, H., Karakas, B., Blair, B.G., Lin, C., et al. (2004). The PIK3CA gene is mutated with high frequency in human breast cancers. *Cancer Biol. Ther.* 3, 772–775.

Bader, G.D., and Hogue, C.W.V. (2003). An automated method for finding molecular complexes in large protein interaction networks. *BMC Bioinformatics* 4, 2.

Bader, G.D., Betel, D., and Hogue, C.W.V. (2003). BIND: the Biomolecular Interaction Network Database. *Nucleic Acids Res.* 31, 248–250.

Bauer, D.E., Hatzivassiliou, G., Zhao, F., Andreadis, C., and Thompson, C.B. (2005). ATP citrate lyase is an important component of cell growth and transformation. *Oncogene* 24, 6314–6322.

Beausoleil, S.A., Jedrychowski, M., Schwartz, D., Elias, J.E., Villén, J., Li, J., Cohn, M.A., Cantley, L.C., and Gygi, S.P. (2004). Large-scale characterization of HeLa cell nuclear phosphoproteins. *Proc. Natl. Acad. Sci. U. S. A.* *101*, 12130–12135.

Ben-Sahra, I., Howell, J.J., Asara, J.M., and Manning, B.D. (2013). Stimulation of de novo pyrimidine synthesis by growth signaling through mTOR and S6K1. *Science* *339*, 1323–1328.

Berwick, D.C., Hers, I., Heesom, K.J., Moule, S.K., and Tavaré, J.M. (2002). The identification of ATP-citrate lyase as a protein kinase B (Akt) substrate in primary adipocytes. *J. Biol. Chem.* *277*, 33895–33900.

Biscardi, J.S., Maa, M.-C., Tice, D.A., Cox, M.E., Leu, T.-H., and Parsons, S.J. (1999). c-Src-mediated Phosphorylation of the Epidermal Growth Factor Receptor on Tyr845 and Tyr1101 Is Associated with Modulation of Receptor Function. *J. Biol. Chem.* *274*, 8335–8343.

Bose, R., Molina, H., Patterson, A.S., Bitok, J.K., Periaswamy, B., Bader, J.S., Pandey, A., and Cole, P.A. (2006). Phosphoproteomic analysis of Her2/neu signaling and inhibition. *Proc. Natl. Acad. Sci.* *103*, 9773–9778.

Cardoso, A.P., Pinto, M.L., Pinto, A.T., Oliveira, M.I., Pinto, M.T., Gonçalves, R., Relvas, J.B., Figueiredo, C., Seruca, R., Mantovani, A., et al. (2014). Macrophages

stimulate gastric and colorectal cancer invasion through EGFR Y1086, c-Src, Erk1/2 and Akt phosphorylation and smallGTPase activity. *Oncogene* 33, 2123–2133.

Cerami, E., Gao, J., Dogrusoz, U., Gross, B.E., Sumer, S.O., Aksoy, B.A., Jacobsen, A., Byrne, C.J., Heuer, M.L., Larsson, E., et al. (2012). The cBio Cancer Genomics Portal: An Open Platform for Exploring Multidimensional Cancer Genomics Data. *Cancer Discov.* 2, 401–404.

Cross, D.A., Alessi, D.R., Cohen, P., Andjelkovich, M., and Hemmings, B.A. (1995). Inhibition of glycogen synthase kinase-3 by insulin mediated by protein kinase B. *Nature* 378, 785–789.

Deckert, M., Elly, C., Altman, A., and Liu, Y.-C. (1998). Coordinated Regulation of the Tyrosine Phosphorylation of Cbl by Fyn and Syk Tyrosine Kinases. *J. Biol. Chem.* 273, 8867–8874.

Dinkel, H., Chica, C., Via, A., Gould, C.M., Jensen, L.J., Gibson, T.J., and Diella, F. (2011). Phospho.ELM: a database of phosphorylation sites--update 2011. *Nucleic Acids Res.* 39, D261–D267.

Fang, W.B., Brantley-Sieders, D.M., Hwang, Y., Ham, A.-J.L., and Chen, J. (2008). Identification and Functional Analysis of Phosphorylated Tyrosine Residues within EphA2 Receptor Tyrosine Kinase. *J. Biol. Chem.* 283, 16017–16026.

Gao, J., Aksoy, B.A., Dogrusoz, U., Dresdner, G., Gross, B., Sumer, S.O., Sun, Y., Jacobsen, A., Sinha, R., Larsson, E., et al. (2013). Integrative Analysis of Complex Cancer Genomics and Clinical Profiles Using the cBioPortal. *Sci. Signal.* *6*, p11–p11.

Goldman, R., Ben Levy, R., Peles, E., and Yarden, Y. (1990). Heterodimerization of the erbB-1 and erbB-2 receptors in human breast carcinoma cells: a mechanism for receptor transregulation. *Biochemistry (Mosc.)* *29*, 11024–11028.

Guryanova, O.A., Wu, Q., Cheng, L., Lathia, J.D., Huang, Z., Yang, J., MacSwords, J., Eyler, C.E., McLendon, R.E., Heddleston, J.M., et al. (2011). Nonreceptor Tyrosine Kinase BMX Maintains Self-Renewal and Tumorigenic Potential of Glioblastoma Stem Cells by Activating STAT3. *Cancer Cell* *19*, 498–511.

Gustin, J.P., Karakas, B., Weiss, M.B., Abukhdeir, A.M., Lauring, J., Garay, J.P., Cosgrove, D., Tamaki, A., Konishi, H., Konishi, Y., et al. (2009). Knockin of mutant PIK3CA activates multiple oncogenic pathways. *Proc. Natl. Acad. Sci.* *106*, 2835–2840.

Hao, Y., Wang, C., Cao, B., Hirsch, B.M., Song, J., Markowitz, S.D., Ewing, R.M., Sedwick, D., Liu, L., Zheng, W., et al. (2013). Gain of interaction with IRS1 by p110 α -helical domain mutants is crucial for their oncogenic functions. *Cancer Cell* *23*, 583–593.

Harsha, H.C., Molina, H., and Pandey, A. (2008). Quantitative proteomics using stable isotope labeling with amino acids in cell culture. *Nat. Protoc.* *3*, 505–516.

Hart, J.R., Liao, L., Yates, J.R., and Vogt, P.K. (2011). Essential role of Stat3 in PI3K-induced oncogenic transformation. *Proc. Natl. Acad. Sci.* *108*, 13247–13252.

Hikri, E., Shpungin, S., and Nir, U. (2009). Hsp90 and a tyrosine embedded in the Hsp90 recognition loop are required for the Fer tyrosine kinase activity. *Cell. Signal.* *21*, 588–596.

Holland, S.J., Gale, N.W., Gish, G.D., Roth, R.A., Songyang, Z., Cantley, L.C., Henkemeyer, M., Yancopoulos, G.D., and Pawson, T. (1997). Juxtamembrane tyrosine residues couple the Eph family receptor EphB2/Nuk to specific SH2 domain proteins in neuronal cells. *EMBO J.* *16*, 3877–3888.

Hornbeck, P.V., Kornhauser, J.M., Tkachev, S., Zhang, B., Skrzypek, E., Murray, B., Latham, V., and Sullivan, M. (2012). PhosphoSitePlus: a comprehensive resource for investigating the structure and function of experimentally determined post-translational modifications in man and mouse. *Nucleic Acids Res.* *40*, D261–D270.

Huang, D.W., Sherman, B.T., and Lempicki, R.A. (2009). Bioinformatics enrichment tools: paths toward the comprehensive functional analysis of large gene lists. *Nucleic Acids Res.* *37*, 1–13.

Huang, W.-C., Chen, Y.-J., Li, L.-Y., Wei, Y.-L., Hsu, S.-C., Tsai, S.-L., Chiu, P.-C., Huang, W.-P., Wang, Y.-N., Chen, C.-H., et al. (2011). Nuclear Translocation of Epidermal Growth Factor Receptor by Akt-dependent Phosphorylation Enhances Breast

Cancer-resistant Protein Expression in Gefitinib-resistant Cells. *J. Biol. Chem.* 286, 20558–20568.

Huse, M., and Kuriyan, J. (2002). The Conformational Plasticity of Protein Kinases. *Cell* 109, 275–282.

Ikenoue, T., Kanai, F., Hikiba, Y., Obata, T., Tanaka, Y., Imamura, J., Ohta, M., Jazag, A., Guleng, B., Tateishi, K., et al. (2005). Functional Analysis of PIK3CA Gene Mutations in Human Colorectal Cancer. *Cancer Res.* 65, 4562–4567.

Jacob, K.K., Whittaker, J., and Stanley, F.M. (2002). Insulin receptor tyrosine kinase activity and phosphorylation of tyrosines 1162 and 1163 are required for insulin-increased prolactin gene expression. *Mol. Cell. Endocrinol.* 186, 7–16.

Janku, F., Wheler, J.J., Naing, A., Falchook, G.S., Hong, D.S., Stepanek, V.M., Fu, S., Piha-Paul, S.A., Lee, J.J., Luthra, R., et al. (2013). PIK3CA Mutation H1047R Is Associated with Response to PI3K/AKT/mTOR Signaling Pathway Inhibitors in Early-Phase Clinical Trials. *Cancer Res.* 73, 276–284.

Jayapandian, M., Chapman, A., Tarcea, V.G., Yu, C., Elkiss, A., Ianni, A., Liu, B., Nandi, A., Santos, C., Andrews, P., et al. (2007). Michigan Molecular Interactions (MiMI): putting the jigsaw puzzle together. *Nucleic Acids Res.* 35, D566–D571.

Jorissen, R.N., Walker, F., Pouliot, N., Garrett, T.P.J., Ward, C.W., and Burgess, A.W. (2003). Epidermal growth factor receptor: mechanisms of activation and signalling. *Exp. Cell Res.* *284*, 31–53.

Kang, S., Bader, A.G., and Vogt, P.K. (2005). Phosphatidylinositol 3-kinase mutations identified in human cancer are oncogenic. *Proc. Natl. Acad. Sci. U. S. A.* *102*, 802–807.

Kerrien, S., Aranda, B., Breuza, L., Bridge, A., Broackes-Carter, F., Chen, C., Duesbury, M., Dumousseau, M., Feuermann, M., Hinz, U., et al. (2012). The IntAct molecular interaction database in 2012. *Nucleic Acids Res.* *40*, D841–D846.

Keshava Prasad, T.S., Goel, R., Kandasamy, K., Keerthikumar, S., Kumar, S., Mathivanan, S., Telikicherla, D., Raju, R., Shafreen, B., Venugopal, A., et al. (2009). Human Protein Reference Database--2009 update. *Nucleic Acids Res.* *37*, D767–D772.

Kosako, H., Yamaguchi, N., Aranami, C., Ushiyama, M., Kose, S., Imamoto, N., Taniguchi, H., Nishida, E., and Hattori, S. (2009). Phosphoproteomics reveals new ERK MAP kinase targets and links ERK to nucleoporin-mediated nuclear transport. *Nat. Struct. Mol. Biol.* *16*, 1026–1035.

Larsen, M.R., Thingholm, T.E., Jensen, O.N., Roepstorff, P., and Jørgensen, T.J.D. (2005). Highly Selective Enrichment of Phosphorylated Peptides from Peptide Mixtures Using Titanium Dioxide Microcolumns. *Mol. Cell. Proteomics* *4*, 873–886.

Laurell, E., Beck, K., Krupina, K., Theerthagiri, G., Bodenmiller, B., Horvath, P., Aebersold, R., Antonin, W., and Kutay, U. (2011). Phosphorylation of Nup98 by multiple kinases is crucial for NPC disassembly during mitotic entry. *Cell* *144*, 539–550.

Le Good, J.A., Ziegler, W.H., Parekh, D.B., Alessi, D.R., Cohen, P., and Parker, P.J. (1998). Protein kinase C isotypes controlled by phosphoinositide 3-kinase through the protein kinase PDK1. *Science* *281*, 2042–2045.

MacGrath, S.M., and Koleske, A.J. (2012). Cortactin in cell migration and cancer at a glance. *J. Cell Sci.* *125*, 1621–1626.

Manning, G., Whyte, D.B., Martinez, R., Hunter, T., and Sudarsanam, S. (2002). The Protein Kinase Complement of the Human Genome. *Science* *298*, 1912–1934.

Martinez-Quiles, N., Ho, H.-Y.H., Kirschner, M.W., Ramesh, N., and Geha, R.S. (2004). Erk/Src phosphorylation of cortactin acts as a switch on-switch off mechanism that controls its ability to activate N-WASP. *Mol. Cell. Biol.* *24*, 5269–5280.

Miao, H., Li, D.-Q., Mukherjee, A., Guo, H., Petty, A., Cutter, J., Basilion, J.P., Sedor, J., Wu, J., Danielpour, D., et al. (2009). EphA2 Mediates Ligand-Dependent Inhibition and Ligand-Independent Promotion of Cell Migration and Invasion via a Reciprocal Regulatory Loop with Akt. *Cancer Cell* *16*, 9–20.

Nakatani, Y., Konishi, H., Vassilev, A., Kurooka, H., Ishiguro, K., Sawada, J., Ikura, T., Korsmeyer, S.J., Qin, J., and Herlitz, A.M. (2005). p600, a unique protein required for membrane morphogenesis and cell survival. *Proc. Natl. Acad. Sci. U. S. A.* *102*, 15093–15098.

Network, T.C.G.A. (2012). Comprehensive molecular portraits of human breast tumours. *Nature* *490*, 61–70.

Newman, R.H., Hu, J., Rho, H.-S., Xie, Z., Woodard, C., Neiswinger, J., Cooper, C., Shirley, M., Clark, H.M., Hu, S., et al. (2013). Construction of human activity-based phosphorylation networks. *Mol. Syst. Biol.* *9*, 655.

Olsen, J.V., Blagoev, B., Gnäd, F., Macek, B., Kumar, C., Mortensen, P., and Mann, M. (2006). Global, In Vivo, and Site-Specific Phosphorylation Dynamics in Signaling Networks. *Cell* *127*, 635–648.

Ong, S.-E., Blagoev, B., Kratchmarova, I., Kristensen, D.B., Steen, H., Pandey, A., and Mann, M. (2002). Stable Isotope Labeling by Amino Acids in Cell Culture, SILAC, as a Simple and Accurate Approach to Expression Proteomics. *Mol. Cell. Proteomics* *1*, 376–386.

Pang, H., Flinn, R., Patsialou, A., Wyckoff, J., Roussos, E.T., Wu, H., Pozzuto, M., Goswami, S., Condeelis, J.S., Bresnick, A.R., et al. (2009). Differential Enhancement of

Breast Cancer Cell Motility and Metastasis by Helical and Kinase Domain Mutations of Class IA Phosphoinositide 3-Kinase. *Cancer Res.* 69, 8868–8876.

Robitaille, A.M., Christen, S., Shimobayashi, M., Cornu, M., Fava, L.L., Moes, S., Prescianotto-Baschong, C., Sauer, U., Jenoe, P., and Hall, M.N. (2013). Quantitative phosphoproteomics reveal mTORC1 activates de novo pyrimidine synthesis. *Science* 339, 1320–1323.

Roovers, K., Wagner, S., Storbeck, C.J., O'Reilly, P., Lo, V., Northey, J.J., Chmielecki, J., Muller, W.J., Siegel, P.M., and Sabourin, L.A. (2009). The Ste20-like kinase SLK is required for ErbB2-driven breast cancer cell motility. *Oncogene* 28, 2839–2848.

Rush, J., Moritz, A., Lee, K.A., Guo, A., Goss, V.L., Spek, E.J., Zhang, H., Zha, X.-M., Polakiewicz, R.D., and Comb, M.J. (2005). Immunoaffinity profiling of tyrosine phosphorylation in cancer cells. *Nat. Biotechnol.* 23, 94–101.

Samuels, Y., Wang, Z., Bardelli, A., Silliman, N., Ptak, J., Szabo, S., Yan, H., Gazdar, A., Powell, S.M., Riggins, G.J., et al. (2004). High Frequency of Mutations of the PIK3CA Gene in Human Cancers. *Science* 304, 554–554.

Samuels, Y., Diaz Jr., L.A., Schmidt-Kittler, O., Cummins, J.M., DeLong, L., Cheong, I., Rago, C., Huso, D.L., Lengauer, C., Kinzler, K.W., et al. (2005). Mutant PIK3CA promotes cell growth and invasion of human cancer cells. *Cancer Cell* 7, 561–573.

Sarbassov, D.D., Guertin, D.A., Ali, S.M., and Sabatini, D.M. (2005). Phosphorylation and Regulation of Akt/PKB by the Rictor-mTOR Complex. *Science* 307, 1098–1101.

Schmidt-Kittler, O., Zhu, J., Yang, J., Liu, G., Hendricks, W., Lengauer, C., Gabelli, S.B., Kinzler, K.W., Vogelstein, B., Huso, D.L., et al. (2010). PI3K α Inhibitors That Inhibit Metastasis. *Oncotarget* 1, 339–348.

Sorkin, A., Waters, C., Overholser, K.A., and Carpenter, G. (1991). Multiple autophosphorylation site mutations of the epidermal growth factor receptor. Analysis of kinase activity and endocytosis. *J. Biol. Chem.* 266, 8355–8362.

Sorkin, A., Helin, K., Waters, C.M., Carpenter, G., and Beguinot, L. (1992). Multiple autophosphorylation sites of the epidermal growth factor receptor are essential for receptor kinase activity and internalization. Contrasting significance of tyrosine 992 in the native and truncated receptors. *J. Biol. Chem.* 267, 8672–8678.

Srivastava, A.K., and Pandey, S.K. (1998). Potential mechanism(s) involved in the regulation of glycogen synthesis by insulin. *Mol. Cell. Biochem.* 182, 135–141.

Swaminathan, S., Kiendl, F., Körner, R., Lupetti, R., Hengst, L., and Melchior, F. (2004). RanGAP1*SUMO1 is phosphorylated at the onset of mitosis and remains associated with RanBP2 upon NPC disassembly. *J. Cell Biol.* 164, 965–971.

Taus, T., Köcher, T., Pichler, P., Paschke, C., Schmidt, A., Henrich, C., and Mechtler, K. (2011). Universal and Confident Phosphorylation Site Localization Using phosphoRS. *J. Proteome Res.* *10*, 5354–5362.

Tice, D.A., Biscardi, J.S., Nickles, A.L., and Parsons, S.J. (1999). Mechanism of biological synergy between cellular Src and epidermal growth factor receptor. *Proc. Natl. Acad. Sci.* *96*, 1415–1420.

Timpson, P., Wilson, A.S., Lehrbach, G.M., Sutherland, R.L., Musgrove, E.A., and Daly, R.J. (2007). Aberrant expression of cortactin in head and neck squamous cell carcinoma cells is associated with enhanced cell proliferation and resistance to the epidermal growth factor receptor inhibitor gefitinib. *Cancer Res.* *67*, 9304–9314.

Ubersax, J.A., and Ferrell, J.E. (2007). Mechanisms of specificity in protein phosphorylation. *Nat. Rev. Mol. Cell Biol.* *8*, 530–541.

Vasudevan, K.M., Barbie, D.A., Davies, M.A., Rabinovsky, R., McNear, C.J., Kim, J.J., Hennessy, B.T., Tseng, H., Pochanard, P., Kim, S.Y., et al. (2009). AKT-Independent Signaling Downstream of Oncogenic PIK3CA Mutations in Human Cancer. *Cancer Cell* *16*, 21–32.

Vivanco, I., and Sawyers, C.L. (2002). The phosphatidylinositol 3-Kinase–AKT pathway in human cancer. *Nat. Rev. Cancer* *2*, 489–501.

Wada, T., Qian, X., and Greene, M.I. (1990). Intermolecular association of the p185neu protein and EGF receptor modulates EGF receptor function. *Cell* *61*, 1339–1347.

Wang, Y., Yang, F., Gritsenko, M.A., Wang, Y., Clauss, T., Liu, T., Shen, Y., Monroe, M.E., Lopez-Ferrer, D., Reno, T., et al. (2011). Reversed-phase chromatography with multiple fraction concatenation strategy for proteome profiling of human MCF10A cells. *PROTEOMICS* *11*, 2019–2026.

Watson, J.A., Fang, M., and Lowenstein, J.M. (1969). Tricarballoylate and hydroxycitrate: substrate and inhibitor of ATP: citrate oxaloacetate lyase. *Arch. Biochem. Biophys.* *135*, 209–217.

Wellen, K.E., Hatzivassiliou, G., Sachdeva, U.M., Bui, T.V., Cross, J.R., and Thompson, C.B. (2009). ATP-citrate lyase links cellular metabolism to histone acetylation. *Science* *324*, 1076–1080.

Wells, C.M., Abo, A., and Ridley, A.J. (2002). PAK4 is activated via PI3K in HGF-stimulated epithelial cells. *J. Cell Sci.* *115*, 3947–3956.

Wilkes, M.C., Mitchell, H., Penheiter, S.G., Doré, J.J., Suzuki, K., Edens, M., Sharma, D.K., Pagano, R.E., and Leof, E.B. (2005). Transforming growth factor-beta activation of phosphatidylinositol 3-kinase is independent of Smad2 and Smad3 and regulates fibroblast responses via p21-activated kinase-2. *Cancer Res.* *65*, 10431–10440.

Wu, G., Xing, M., Mambo, E., Huang, X., Liu, J., Guo, Z., Chatterjee, A., Goldenberg, D., Gollin, S.M., Sukumar, S., et al. (2005). Somatic mutation and gain of copy number of PIK3CA in human breast cancer. *Breast Cancer Res. BCR* 7, R609–R616.

Wu, X., Renuse, S., Sahasrabudde, N.A., Zahari, M.S., Chaerkady, R., Kim, M.-S., Nirujogi, R.S., Mohseni, M., Kumar, P., Raju, R., et al. (2014). Activation of diverse signalling pathways by oncogenic PIK3CA mutations. *Nat. Commun.* 5.

Wybenga-Groot, L.E., Baskin, B., Ong, S.H., Tong, J., Pawson, T., and Sicheri, F. (2001). Structural Basis for Autoinhibition of the EphB2 Receptor Tyrosine Kinase by the Unphosphorylated Juxtamembrane Region. *Cell* 106, 745–757.

Xue, G., and Hemmings, B.A. (2013). PKB/Akt-dependent regulation of cell motility. *J. Natl. Cancer Inst.* 105, 393–404.

Yokoyama, N., and Miller, W.T. (2003). Biochemical Properties of the Cdc42-associated Tyrosine Kinase ACK1 SUBSTRATE SPECIFICITY, AUTOPHOSPHORYLATION, AND INTERACTION WITH Hck. *J. Biol. Chem.* 278, 47713–47723.

Yokoyama, N., and Miller, W.T. (2006). Purification and Enzyme Activity of ACK1. In *Methods in Enzymology*, C.J.D. and A.H. William E. Balch, ed. (Academic Press), pp. 250–260.

Yoon, S.-O., Shin, S., Liu, Y., Ballif, B.A., Woo, M.S., Gygi, S.P., and Blenis, J. (2008). Ran-binding protein 3 phosphorylation links the Ras and PI3-kinase pathways to nucleocytoplasmic transport. *Mol. Cell* *29*, 362–375.

Yu, J., Zhang, Y., McIlroy, J., Rordorf-Nikolic, T., Orr, G.A., and Backer, J.M. (1998). Regulation of the p85/p110 Phosphatidylinositol 3'-Kinase: Stabilization and Inhibition of the p110 α Catalytic Subunit by the p85 Regulatory Subunit. *Mol. Cell. Biol.* *18*, 1379–1387.

Yuan, J., Luo, K., Zhang, L., Cheville, J.C., and Lou, Z. (2010). USP10 regulates p53 localization and stability by deubiquitinating p53. *Cell* *140*, 384–396.

Zahari, M.S., Wu, X., Blair, B.G., Pinto, S.M., Nirujogi, R.S., Jelinek, C.A., Malhotra, R., Kim, M.-S., Park, B.H., and Pandey, A. (2015). Activating Mutations in PIK3CA Lead to Widespread Modulation of the Tyrosine Phosphoproteome. *J. Proteome Res.*

Zhang, L., Lubin, A., Chen, H., Sun, Z., and Gong, F. (2012). The deubiquitinating protein USP24 interacts with DDB2 and regulates DDB2 stability. *Cell Cycle Georget. Tex* *11*, 4378–4384.

Zhao, L., and Vogt, P.K. (2008). Helical domain and kinase domain mutations in p110 α of phosphatidylinositol 3-kinase induce gain of function by different mechanisms. *Proc. Natl. Acad. Sci.* *105*, 2652–2657.

Zhao, J.J., Liu, Z., Wang, L., Shin, E., Loda, M.F., and Roberts, T.M. (2005). The oncogenic properties of mutant p110 α and p110 β phosphatidylinositol 3-kinases in human mammary epithelial cells. *Proc. Natl. Acad. Sci. U. S. A.* *102*, 18443–18448.

Zhao, M., Xia, L., and Chen, G.-Q. (2012). Protein kinase c δ in apoptosis: a brief overview. *Arch. Immunol. Ther. Exp. (Warsz.)* *60*, 361–372.

Curriculum Vita

Muhammad Saddiq Zahari

ADDRESS Department of Biological Chemistry
The Johns Hopkins University School of Medicine
733 North Broadway, Broadway Research Building 560
Baltimore, Maryland, USA 21205

TELEPHONE (410)336-2422

E-MAIL mzahari2@jhmi.edu

BIRTH 05/26/1985 Ipoh, Perak, Malaysia

EDUCATION

Doctor of Philosophy, 2015

Department of Biological Chemistry, Johns Hopkins University School of Medicine,
Baltimore, Maryland, USA

Master of Arts, 2010

Graduate School of Arts & Sciences, Columbia University in the City of New York, USA

Bachelor of Science, 2008

School of Biosciences, The University of Nottingham, UK

TEACHING EXPERIENCE

2010 – 2011 Research assistant, Perdana University Graduate School of Medicine,
Malaysia

PUBLICATIONS (peer-reviewed original articles)

Zahari M. S.*, Wu X.*, Blair B. G., Kim M. S., Pinto S. M., Nirujogi R. S., Jelinek C. A., Malhotra R., Park B. H., Pandey A. (2015) Activating mutations in PIK3CA result in widespread modulation of the tyrosine phosphoproteome. *Journal of Proteome Research*. 14, 3882-3891 *equal contribution

Zahari M. S.*, Wu X.*, Pinto S. M., Nirujogi R. S., Fetics B., Philip M., Barnes S. R., Godfrey B., Gabrielson E., Nevo E., Pandey A. (2015) Phosphoproteomic profiling of tumor tissues identifies HSP27 Ser82 phosphorylation as a robust marker of early ischemia. *Scientific Reports*. 5, 13660 *equal contribution

Wu X.*, **Zahari M. S.***, Renuse S., Nirujogi R. S., Kim M. S., Manda S. S., Stearns V., Gabrielson E., Sukumar S. and Pandey A. (2015) Phosphoproteomic analysis identifies FAK2 as a potential therapeutic target for tamoxifen resistance in breast cancer. *Molecular & Cellular Proteomics*. 2015 Sep 3 *equal contribution

Wu X.*, **Zahari M. S.***, Ma B., Liu R., Renuse S., Sahasrabudhe N.A., Chen L., Chaerkady R., Kim M.S., Zhong J., Jelinek C., Barbhuiya M. A., Leal-Rojas P., Yang Y., Kashyap M. K., Marimuthu A., Ling M., Fackler M. J., Merino V., Zhang Z., Zahnow C. A., Gabrielson E., Stearns V., Sukumar S., Gill P. and Pandey A. (2015) Global phosphotyrosine survey in triple negative breast cancer reveals activation of multiple tyrosine kinase signaling pathways. *Oncotarget*. 6, 29143-29160 *equal contribution

Wu, X*., **Zahari, M. S.***, Renuse, S., Sakamuri, S., Singal, M., Gabrielson, E., Sukumar, S. and Pandey, A. (2014). A breast cancer cell microarray (CMA) as a rapid method to characterize candidate biomarkers. *Cancer Biology and Therapy*. 15, 1593-1599. *equal contribution

Wu, X., Renuse, S., Sahasrabudde, N. A., **Zahari, M. S.**, Chaerkady, R., Kim, M. S., Nirujogi, R. S., Mohseni, M., Kumar, P., Raju, R., Zhong, J., Yang, J., Neiswinger, J., Jeong, J. S., Newman, R., Powers, M. A., Somani, B. L., Gabrielson, E., Sukumar, S., Stearns, V., Qian, J., Zhu, H., Vogelstein, B., Park, B. H. and Pandey, A. (2014). Activation of diverse signaling pathways by oncogenic PIK3CA mutations. *Nature Communications*. 5, 4961

Blair, B. G., Wu, X., **Zahari, M. S.**, Mohseni, M., Cidado, J., Wong, H. Y., Beaver, J. A., Cochran, R. L., Zabransky, D. J., Croessmann S., Chu, D., Toro, P.V., Cravero, K., Pandey, A. and Park, B. H. (2015). A phosphoproteomic screen demonstrates differential dependence on HER3 for MAP kinase pathway activation by distinct PIK3CA mutations. *Proteomics*. 15, 318-326

Kim, M. S., Pinto, S. M., Getnet, D., Nirujogi, R. S., Manda, S. S., Chaerkady, R., Madugundu, A. K., Kelkar, D. S., Isserlin, R., Jain, S., Thomas, J. K., Muthusamy, B., Leal-Rojas, P., Kumar, P., Sahasrabudde, N. A., Balakrishnan, L., Advani, J., George, B., Renuse, S., Selvan, L. D. N., Patil, A. H., Nanjappa, V., Radhakrishnan, A., Prasad, S., Subbannayya, T., Raju, R., Kumar, M., Sreenivasamurthy, S. K., Marimuthu, A., Sathe, G. J., Chavan, S., Datta, K. K., Subbannayya, Y., Sahu, A., Yelamanchi, S. D., Jayaram, S., Rajagopalan, P., Sharma, J., Murthy, K. R., Syed, N., Goel, R., Khan, A. A., Ahmad, S., Dey, G., Mudgal, K., Chatterjee, A., Huang, T. C., Zhong, J., Wu, X., Shaw, P. G., Freed, D., **Zahari, M. S.**, Mukherjee, K. K., Shankar, S., Mahadevan, A., Lam, H., Mitchell, C. J., Shankar, S. K., Satishchandra, P., Schroeder, J. T., Sirdeshmukh, R., Maitra, A., Leach, S. D., Drake, C. G., Halushka, M. K., Prasad, T. S. K., Hruban, R. H.,

Kerr, C. L., Bader, G. D., Iacobuzio-Donahue, C. A., Gowda, H. and Pandey, A. (2014).
A draft map of the human proteome. *Nature*. 509, 575-581.